X-ray Diffraction

Studies of Substituted Thiourea Complexes of Coinage Metals

The University of Manchester

School of Chemistry

MSc by Research

Chemistry

2010-2011

Amjad Farooq Amjad

Table of Content

Abbreviations

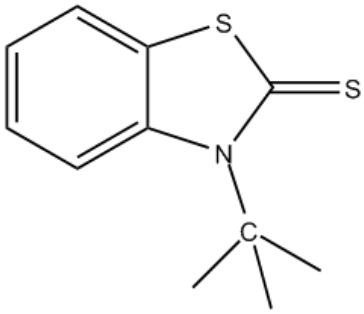

$C_8H_7NS_2$

3-methylbenzothiazole-2-thione (mbtt)

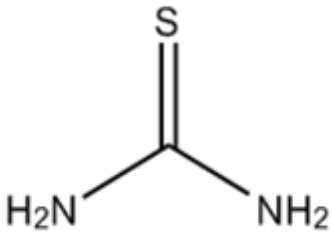

NH_4SCN

thiourea (tu)

$AgNO_3$

Silver Nitrate

Cu(I)Cl

Cuprous Chloride

CH_3OH

Methanol

CH_3COCH_3

Acetone

Abstract

In this work the fundamental techniques to study the structure of complexes have been discussed. An overview of crystallography and X-ray diffraction is provided to study the complexes.

A study of coinage metals like copper and silver bound to substituted thiourea was proposed. Copper was used as Cu(I)Cl and silver was used as $AgNO_3$. Thiourea (tu) and 3-methylbenzothiazole-2-thione (mbtt) have been used as ligands. The reactions were carried out under mild conditions and at a very low concentration of 0.01M. Different solvents were used to prepare solutions. Typically the effect of very low concentration and the use of different solvents on the nature of the product were analysed.

The copper complexes like complex 1, $\mu_2Cl_2[Cu_2(mbtt)_4]$, complex 3, Di-2-thienylmethanone, complex 4 between Cu(I)thiourea and Silver complex 2, $[Ag(mbtt)(NO_3)]_n$ have been synthesized and structurally characterised. The complex 1, complex 2 and complex 3 have been characterised by single crystal X-ray diffraction. X-ray powder diffraction has been used in the characterisation of complex 4.

The crystal structure of all these complexes have been determined and not found in crystallographic data. It was found that the complexes show different polymeric and dimeric formation depending on the conditions employed. The structure of the complexes has been explained on the basis of intermolecular forces.

Declaration

I hereby declare that this thesis is my own work and effort and that it has not been submitted anywhere for any award. I declare that no part of this dissertation has been taken from existing published or unpublished material without due acknowledgement and that all secondary material used therein has been fully referenced.

SIGNED: ……

DATE: …….

Copyright Statement

Acknowledgement

All Praise ultimately belongs to Allah the Almighty on Whom we depend for sustenance and guidance. And I thank Allah for giving me the strength and guidance for completing my work accordingly.

I wish to express my sincere gratitude to Dr. Robin Pritchard for providing me an opportunity to do my research work on:

"X-ray Diffraction Studies of Substituted Thiourea Complexes with Coinage Metals".

I sincerely thank my colleagues too who rendered their help during my work. Had it not been for their kind co-operation things would be much harder for me during this research project.

I wish to avail myself of this opportunity to express a sense of gratitude and love to my friends and my beloved family for providing me the right environment and the moral support I needed for my work.

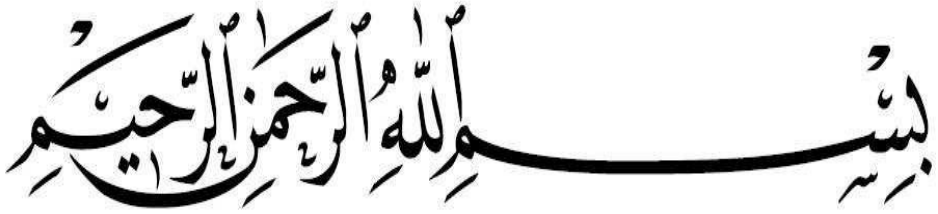

In the Name of Allāh, the Most Gracious, the Most Merciful

Chapter 1

Basic Concepts and Fundamental Techniques

1. Introduction

The complex structures of coinage metals (Ag, Cu) with thiourea and substituted thiourea[1-3] have been synthesized for a long time. These complexes are synthesized due to their well prominent structural behaviour. On the other hand the formation of these complexes has been remarked for their potential aspects in many fields and has become an important part of optical, electrical, magnetic materials etc. Similarly these complexes have been used in antiviral and antibacterial drugs to show their importance in the pharmaceutical industry.

The behaviour of these complexes mainly depends on the types, structures and the binding site of functional groups of the ligand. Thiourea or substituted thiourea is a ligand which contains different sites for bonding like N and S atoms. The coinage metals have the ability to form coordinate covalent bonds either via both the sulphur and nitrogen or via one of these atoms.

It has been reported in the recent papers that heterocyclic thioamides[4-6] show a tendency to form complexes like polymers and dimers. The synthesis of these complexes includes variable coordination of sulphur, nitrogen and contribution of halogen donor atoms.

These coordinating complexes form an essential constituent of research in inorganic chemistry for developing new functional materials like organometallics and shows their possible applications in different fields of chemistry like crystal engineering, super molecular chemistry, isomerisation, and nano chemistry.

In view of the applications of these complexes in daily life and different fields of chemistry, this research was undertaken.

In the present research project certain changes have been made to form the complexes to study their effects on the products. Especially the following steps have been taken that effect the formation of the product:

- Different solvents are used for solution making
- Prepare the solutions of very low concentrations like 0.01M
- Salts of Cu(I)Cl, $Ag(I)NO_3$ are directly used to form the solution

- At some point products are re-crystallised to check the morphology
- Methanol(dry), acetone, acetonitrile are used as solvents

1.1 Thiourea

Thiourea is a white crystalline solid[7]**.** It is named as 2-thiourea; thiocarbamide, sulfourea. It occurs in two tautomers as given in eqn.1.1. It contains functional groups as amino group, imino group, and thiol group as shown in eqn. 1.1.

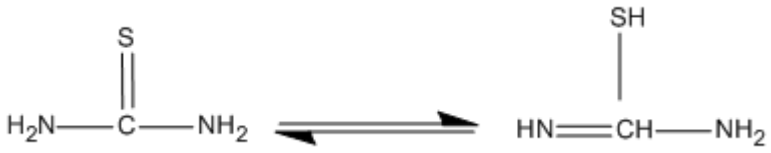

Eqn. 1.1 Tautomers of thiourea

It does not have any sharp melting point, as at a temperature of 135 °C it is converted to ammonium thiocyanate (NH_4SCN).

It is an organic compound soluble in aprotic organic solvent and polar protic solvent. It is insoluble in non-polar solvent. It is soluble in water at 20 ^{0}C. It is studied by HPLC chromatography and by following UV spectroscopy. It shows an absorption maximum at 238 nm. It was measured in water having a pH 7.4.

Following are some of the areas where thiourea has an extensive series of uses:

1. Production and change of textile as well as dyeing
2. Production and alteration of synthetic resins
3. Manufacturing of pharmaceuticals such as sulfathiazole's etc.
4. Manufacturing of industrial cleaning agents and engraving metal surfaces
5. Elimination of metals like mercury from waste water
6. Refinement, electrolysis, electroplating, extraction of metals like Cu, Ag etc.
7. In photography it is used for image reproduction
8. In biochemistry it is used as anti-oxidant agent

Thiourea behaves as a "soft" ligand, capable of forming unidentate, multidentate or diverse bridging modes in its complexes with coinage metal salts. i.e. Cu(I)Cl, $AgNO_3$, AgBr, CuSCN, Cu(II)Cl_2 . These associated "hard" anions usually being excluded from the coordination sphere while "soft" anions such as the heavier halide ions may be competitive. For crystallization from varied solvents, the strong hydrogen-bonding, rearrangements of complexes, capable of modification by substitution, may be relevant. Already a number of structures for thiourea and substituted thiourea like heterocyclic compounds with copper and silver salts with simple "hard" or "soft" groups (halide X = Cl, Br, I & X = SCN, CN, NO_3) have been discussed in the literature[8]. Practically such complexes can play a role:

1. In copper electroplating as a levelling agent
2. As an inhibitor for copper oxidization in brutal aqueous atmospheres.

1.2 Coinage Metals:

The three malleable ductile transition metals copper, silver, gold are known as coinage metals. In the periodic table these metals are placed in group 11 with their outer electronic configurations $nd^{10}(n+1)s^1$. These metals are difficult to oxidize and are resistant to corrosion due to having high ionization potentials and higher standard electrode potentials.

A range of metal-thiourea complexes on the basis of ligand bonding mode has been reported[4-6]**.** This project will provide the detail knowledge of syntheses and crystal structures of new or existing complexes with organic ligands. It was mainly interesting to find out what the applications of these species are:

- Luminescent materials (due to $d^{10} \rightarrow d^9p^1$ orbital interactions)[9] for metal film deposition
- Silver is used as in anti-tumour agent
- Rigid-rod polymers having extensive delocalisation along their backbones

Copper(I)Chloride: CuCl

Copper chloride is a white solid readily oxidized to pale green colour. It is known as cuprous chloride, is the lower chloride of copper. It is sparingly soluble in water, but quickly soluble in concentrated hydrochloric acid. (Fig.1.1)

Fig. 1.1 Different forms of copper (I) chloride
over copper wire, powder compound and crystal structure

Silver Nitrate: $AgNO_3$

It is an inorganic compound having formula $AgNO_3$. It is sensitive to light. $AgNO_3$ is a white crystalline solid as shown in fig. 1.2.

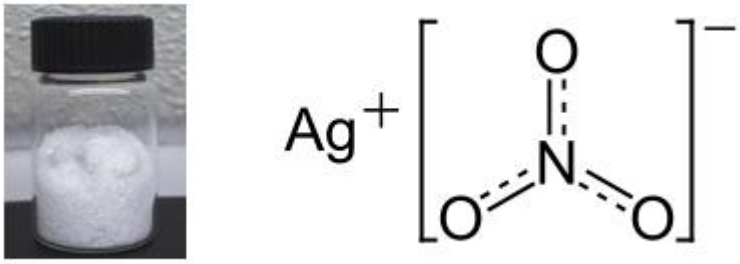

Fig. 1.2 White crystals of silver nitrate

Aims of Research Project

This project was undertaken to study the coordination of coinage metals with substituted thioureas. There are two aspects of this study:

- Synthesis of the complexes
- Analysis and characterization of their structures.

The current research is intended to extend our knowledge of the complex chemistry of coinage metals. In particular the effect of mild synthesis conditions and low reagent concentration on the formation of the products will be explored.

A survey of the Cambridge Crystallographic Database will be carried out initially to identify suitable ligand types. This will be followed by powder XRD to screen for novel complexes and finally single crystal analysis to fully characterise the structures.

1.3 Structural Characterization Techniques

Chemists employ two main structural characterisation techniques to demonstrate the structure of a compound.

1.3.1 Spectroscopy

This technique measures the photons that are absorbed during molecular transitions. The appearance of the spectra depends on the type of chemical species present and molecular symmetry. Infrared, Raman, NMR and EPR spectroscopy have been employed for this purpose. This method can be used on liquids and amorphous solids.

1.3.2 Diffraction

Diffraction occurs when waves are scattered by objects whose separation is comparable to the wave's wavelength. These waves then either cancel the effect of each other to give destructive interference or reinforce each other to give constructive interference. This method is primarily used on crystalline solids. However diffraction can also be used on amorphous solids (EXAFS) and gases (Gas Phase Electron Diffraction) to provide important structural information.

In the 2-dimensional case two constructive interference conditions have to be satisfied simultaneously so light regions reduced.

Crystals behave as 3-dimensional diffraction gratings when illuminated with X-rays (wavelength similar to atomic separation). In this case three constructive interference conditions have to be satisfied simultaneously so that the diffraction pattern produced when a stationary crystal is illuminated by monochromatic X-rays is extremely sparse.

Diffraction patterns can be measured accurately using a single crystal diffractometer and transformed into a high resolution 3D molecular structure using crystallographic software to identify the structure of a compound.

Certain techniques are used to understand the structure of compound and crystallography is one of the most advanced tools used for structure elucidation**.** If the crystal is a suitable size ($0.1 \times 0.1 \times 0.1$ mm^3) then single crystal methods are used however if the crystals are too small useful structure information can be obtained by powder diffraction techniques. On this basis X-ray powder diffraction and single crystal X-ray diffraction are used to provide structural information and even show the complete structure of a compound.

These techniques operate in combination with some others to solve the full structure of a compound. So, to understand crystallography we have to understand these techniques and how they combine to make modern X-ray diffraction such a powerful method. Similarly a range of software is used to identify, refine the structure of a compound as well as compare it with other crystal structures which are linked to each other.

1.3.3. Crystallography

It is the science of crystals, which is dedicated to the study of their reaction and growth, their external form, internal structure and physical properties. For the development of effective drugs the information of exact molecular structures of a compound is needed for drug design and structure based focused studies. Many structure related questions can be answered regularly by crystallography from global folds in proteins to atomic details of bonding. Unlike NMR spectroscopy, crystallography has no size limitation to the molecule to be examined. The price for the high accuracy of crystallographic structure is that a good crystal must be grown,

and that only limited information about the molecules dynamic behaviour in solution is available from one single diffraction experiment.
In the beginning it was regarded as a part of mineralogy. However, on the basis of the following reasons, it became an independent discipline, which is as follow:

- Due to research progress in chemistry, it was proved that in a wide range of substance, having nothing in common with minerals having crystalline structures.
- Crystals have very diverse and precise properties.

To develop the better understanding of fundamental concepts of X-ray diffraction, the types of solid matter should be distinguished, and the possible description could be like:

- Amorphous solids: The atoms are ordered in an arbitrary way as they are ordered in liquids and glasses.
- Crystalline solids: regular pattern is designed for atoms in crystalline solids.

95% of all solid material can be described as crystalline. Hence a method capable of studying crystalline solids is very important to the chemist and will have widespread use to deduce the structure of a newly formed compound in a short time.

1.4. The nature and production of X-rays

X-rays are electromagnetic radiation having wavelength in the range of 0.01nm to 10 nm and energies in the range 120 eV to 120 keV. X-rays are smaller in wavelength than UV and longer than γ-rays. These rays occupy a region in an electromagnetic spectrum between γ -rays and ultraviolet (UV) as shown in fig.1.3.

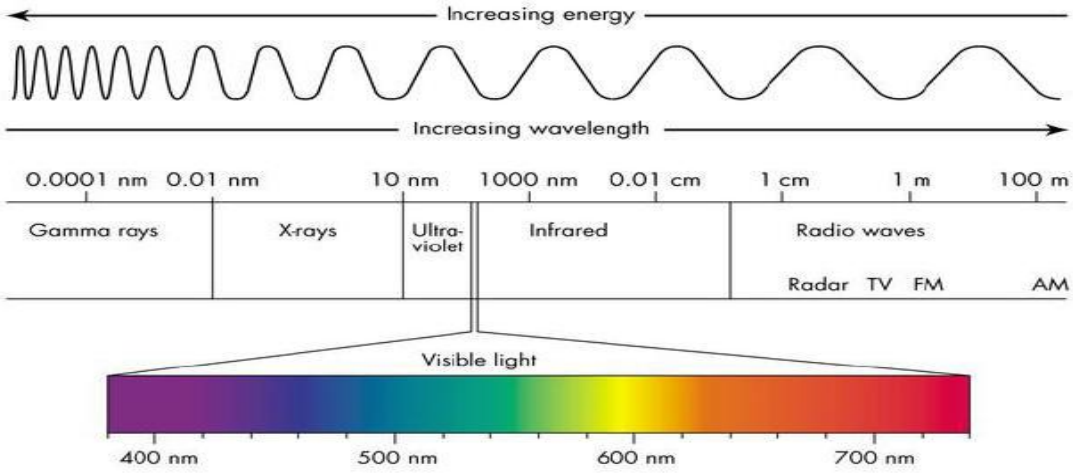

Fig. 1.3 Electromagnetic spectrum of light

Monochromatic X-rays are required for diffraction applications. These are created by accelerating electrons through a potential difference in the range 40-60kV and by using a metal such as Cu as a target as shown in fig.1.4 which emits X-ray of characteristic wavelength λ 1.5418Å.

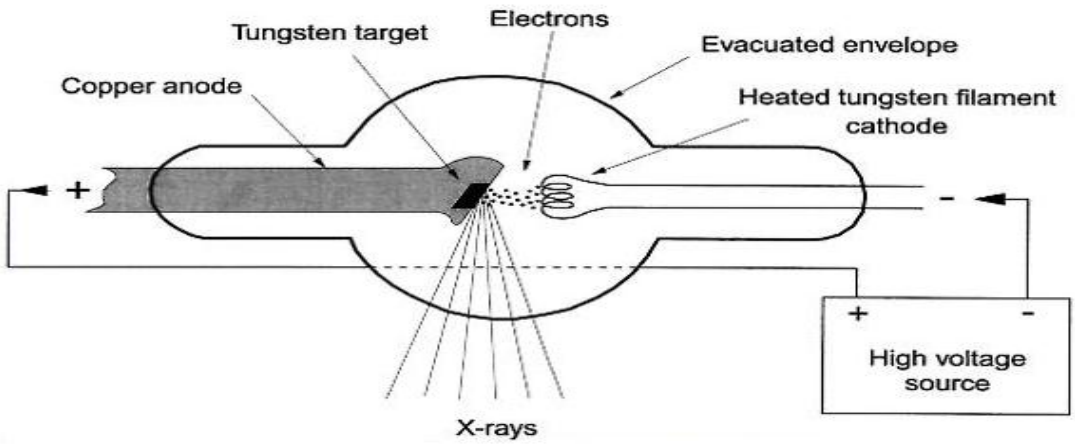

Fig. 1.4 Apparatus for X-ray production

In addition, as electrons collide with the target atoms they slow down and produce a continuous spectrum of X-rays which are termed Bremsstrahlung radiation.

In order to produce monochromatic X-rays this beam of radiation is directed on to a crystal of graphite oriented in such a way that only the chosen wavelength fulfils the Bragg's equation. Only this wavelength is diffracted, allowing the rest of the radiation to pass through the monochromator crystal.

The wavelength of X-rays are comparable to the atom's size so these rays diffract well and ideal for resolving the structural arrangement of atoms and molecule in the crystal. The active X-rays pierce deep into the materials and give facts about the bulk structure.

Recently synchrotron facilities become ideal sources for the measurements X-ray diffraction**.** X-rays radiations are emitted by electrons or positrons that are travelling almost with the speed of light in a ring of circular storage. Synchrotron radiations are more powerful and intense in comparison to X-ray tubes, so it has become important equipment for a broad range of structural inquiries and brought developments in numerous fields of science and technology.

1.4.1. The Basics of Diffraction

Diffraction is the slight turning of light around the edge of a sharp object as it passes through. The magnitude of the turning depends on the relative size of the wavelength.

Objects are visible because they scatter the light falling on them. Actually light consists of waves and each scattered wave has a particular intensity and phase relative to other scattered waves which results from the scattering that produced it. The scattered rays from various objects can interfere with each other and the resulting intensity distribution is strongly controlled by this interaction to create an image for observation. So information about the shape of an object can be deduced from the knowledge of the intensities and phase of scattered waves. The scattering of

visible light is effectively negligible at atomic level, because of the relative wavelength of light .i.e. (400nm-700nm).

X-rays are used to overcome this problem, so only Hard X-rays are used. But as the physical reunion of the scattered X-rays to form an image is not possible, study of objects at atomic levels is not a simple matter. A photographic film or detector is used to record the pattern of the scattered X-rays. The overall process of recombination can be handled by a series of mathematical techniques. These techniques make use of the relationship between the object and its scattering pattern to carry out structure determinations.

1.4.2. X-ray Diffraction

X-ray diffraction is a fundamental and non-destructive analysis technique. Different patterns could be generated with the interaction of X-rays and crystalline substance. A unique pattern is obtained from each crystalline matter:

"The same substance always gives the same pattern and in a mixture of substances each produces its pattern separately of the others[10]."

Therefore the X-ray diffraction pattern of a substance is like an impression of the substance. The powder diffraction technique is thus ideal for the depiction and identification of poly-crystalline phases.

So for approximately 50,000 inorganic and 25,000 organic single components crystalline phase diffraction patterns have been stored on magnetic or optical media as standards

So, X-ray crystallography is an experimental technique not only an imaging technique. It looks into the fact that X-rays are diffracted by crystals which have the appropriate wavelength~10^{-8}cm to be scattered by the electron cloud of an atom. The electron density can be remodelled based on the diffraction pattern attained from X-ray scattering off the periodic assembly of atoms in the crystal. Additional phase

information must be extracted either from the diffraction data or from supplementing diffraction experiments to complete the reconstruction. A model is then gradually built into the experimental electron density, refined against the data and the result is a quite accurate molecular structure.

1.5. X-rays diffraction and crystal system

In an alternating electromagnetic field an electron will oscillate with the same frequency as the field. When an atom is hit by an X-ray beam, the electrons around the atom start to vibrate with the same frequency as the incoming beam. As a result destructive interference is produced in all directions, i.e., no resultant energy leaving the solid sample as the combining waves are out of phase. However the atoms in a crystal are orderly in a regular pattern, and in a very few directions will give constructive interference. The waves will be in phase and there will be distinct X-ray beams leaving the sample in all possible directions. Hence, a diffracted beam may be termed as a beam consisting of a large number of scattered rays mutually strengthening one another.

Some basic fundamentals are required to understand how to abstract the structural information of a compound from the diffraction pattern. These are described below step by step.

Basic Crystallographic terms

1. Unit cell
2. Crystal system
3. Crystal centring
4. Miller indices
5. Bragg's law

6. Symmetry
7. Intensities of diffracted X-rays
8. Phase problem
9. Solving the Phase problem
10. Refining and completing structure
11. R-factors
12. Location of atoms in the unit-cell

1.5.1. Unit cell

The basic structure block of a periodic crystal, which when repeated "infinitely" in three dimensions produces a macroscopic crystal. The entire crystal is generated when the unit cell is repeated periodically according to the translation vectors of the crystal lattice. The crystals[11] are built up of a regular arrangement of atoms in 3D being represented by the repeating unit as shown in fig.1.4. The smallest volume element that shows the full symmetry of the crystal unit is called a unit cell. The replication of the unit cell is effectively infinite on the atomic scale. It is characterized by three vectors a, b and c, that form the edge of a parallelepiped and the angles between them,α, β and γ. The repeat can be portrayed using a crystal lattice. Each unit cell contains the equivalent of one lattice point.

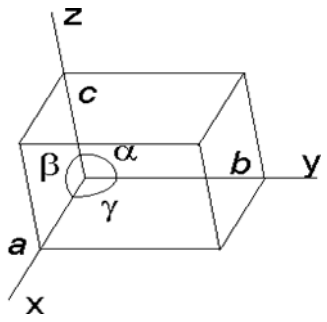

Fig. 1.4 A single crystal unit

1.5.2. Crystal system

The seven crystal systems, classified in terms of their minimum symmetry, correspond to the seven fundamental shapes for unit cells as shown in fig. 1.5. The higher a unit cell symmetry, the higher the symmetry of the atomic and molecular arrangements that can be accommodated within that cell.

Table 1.1

Crystal System with unit cell symmetry

Crystal System	Unit cell shape	Characteristic minimum symmetry axis
Triclinic or Anorthic	$a \neq b \neq c$ and $\alpha \neq \beta \neq \gamma \neq 90^o$	None
Monoclinic	$a \neq b \neq c$, $\alpha = \gamma = 90^o$ and $\beta \neq 90^o$	2-fold
Orthorhombic	$a \neq b \neq c$ and $\alpha = \beta = \gamma = 90^o$	Three 2-fold at 90^o
Tetragonal	$a = b \neq c$ and $\alpha = \beta = \gamma = 90^o$	4-fold
Hexagonal	$a = b \neq c$, $\alpha = \beta = 90^o$ and $\gamma = 120^o$	6-fold
Rhombohedral or Trigonal	$a = b = c$ and $\alpha = \beta = \gamma \neq 90^o$	3-fold
Cubic	$a = b = c$ and $\alpha = \beta = \gamma = 90^o$	Four 3-fold at 109.47^o

1.5.3. Crystal Centering

Some of the crystal systems can be centred:-

- Primitive i.e. no centre (P)
- Body-centred (I)
- Face centred i.e. all the faces centred (F)
- One centred face (A, B or C)
- Rhombohedral indexed on hexagonal axes (R) i.e. can choose P or R for Rhombohedral, do not need both.

Fourteen Bravais lattices are sufficient to describe all crystal structures. (Table. 1.2)

Table 1.2 Bravais lattices for crystal centering

Crystal System	Centring
Triclinic or Anorthic	P
Monoclinic	P, C
Orthorhombic	P, C, I, F
Tetragonal	P, I
Hexagonal	P
Rhombohedral or Trigonal	P/R (R if hexagonal axes chosen)
Cubic	P, I, F

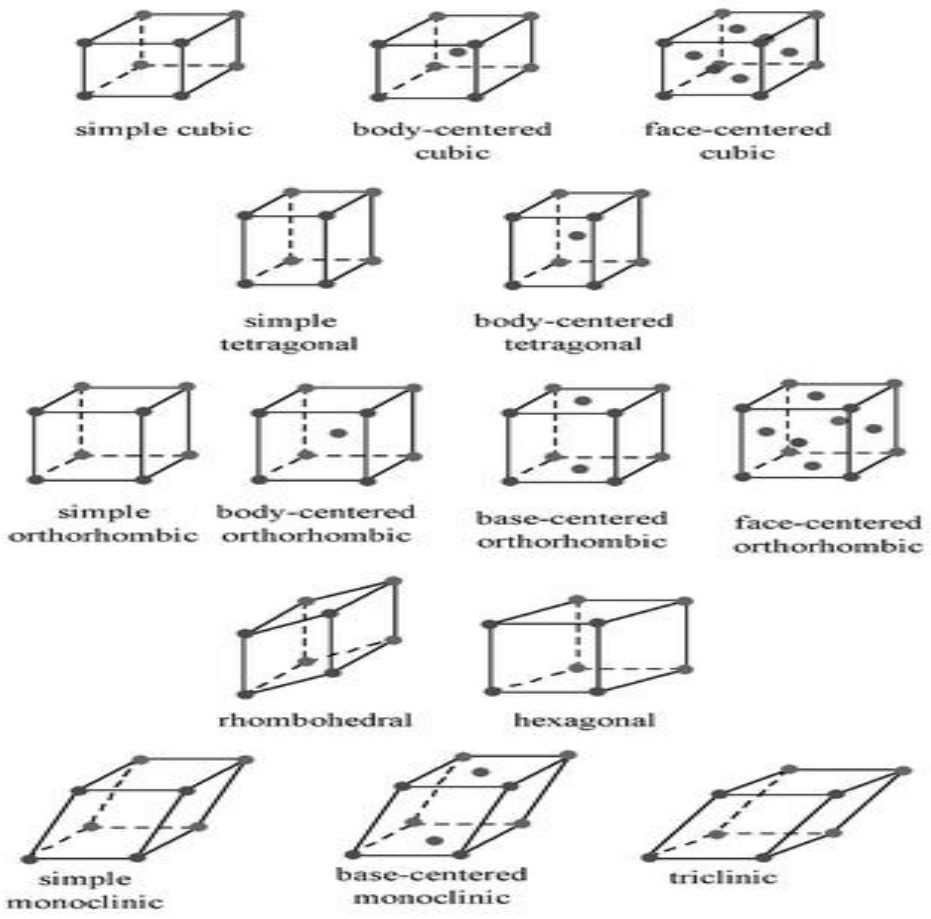

Fig. 1.5 Bravais Lattices for seven crystal system

1.5.4. Miller indices

In crystal structures it is important to be able to specify a plane or a set of planes in the crystal. Planes in a crystal can be specified using a notation called Miller indices. The Miller index is indicated by the notation [*hkl*] where *h*, *k*, and *l* are reciprocals of the plane with the *x*, *y*, and *z* axes. The plane with Miller indices h, k and l makes intercepts a/h, b/k and c/l with the unit-cell axes a, b and c as shown in fig. 1.6. Reflection files contain lists of h, k, l, I and σ(I).

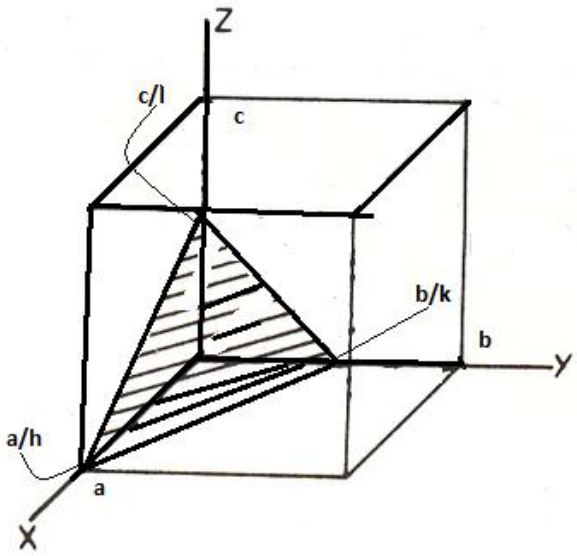

Fig. 1.6 Plane with Miller indices

There are certain steps to calculate the Miller indices. These are:

- The plane to be calculated is located on a unit cell
- The intercepts are calculated with each of the crystal axes
- Then reciprocal of the intercepts are considered
- The above calculated parameters are then multiplied by a scalar number to make sure that the simple ratios are converted to whole numbers

Miller indices[11] can be explained by using a simple example as given in fig.1.6a. The face along x-axis of a lattice where y-axis or z-axis does not intersect would be plane (100), while a plane along the body diagonal would be the (111). Similarly by applying the same method the other plane (110) can be calculated.

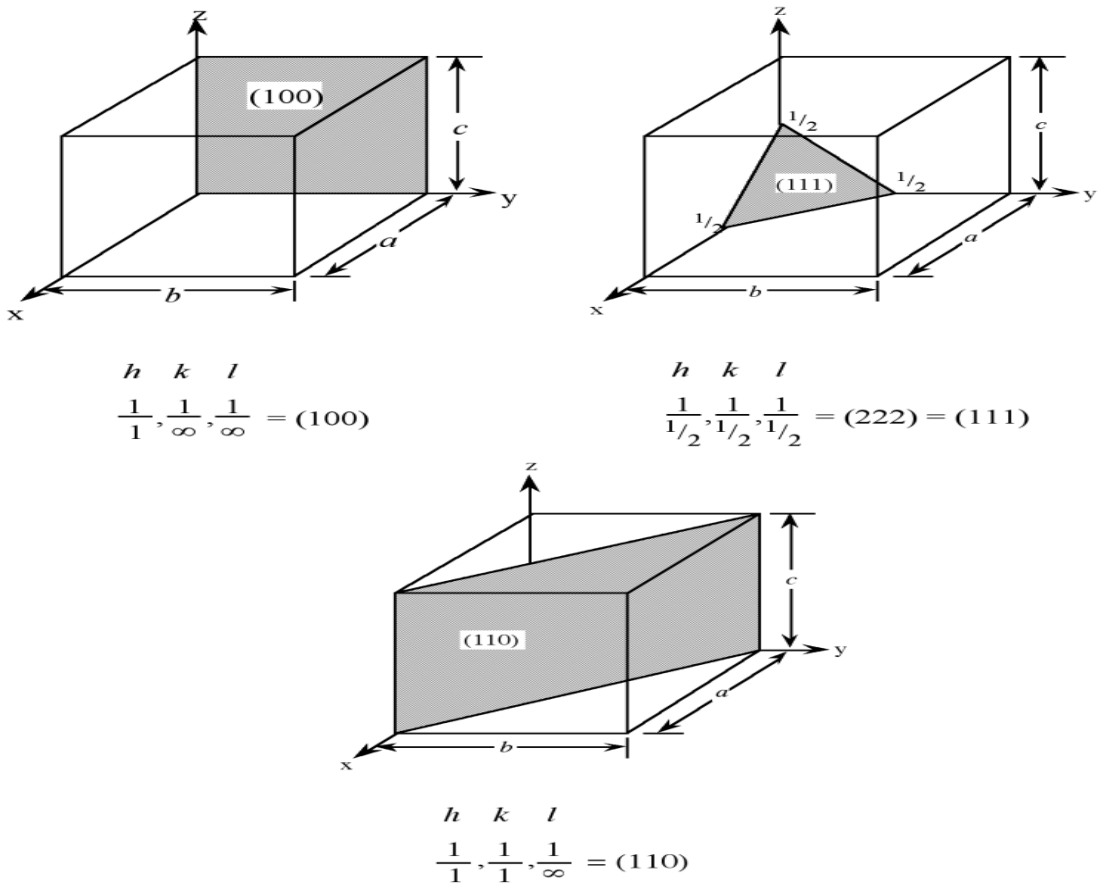

Fig. 1.6a Plane with Miller indices for a cubic lattice

Miller indices directions may be grouped in families in crystal directions. Miller indices are given in parentheses (*hkl*), while braces {*hkl*} are placed around the indices of a family of planes. e.g. (001), (100), and (010) are all in the {100} family of planes, for a cubic lattice.

1.5.5. Bragg's Law

Bragg[12] found that crystalline materials gave typical patterns of intense reflected X-ray intensity peaks. He gave a simple concept to explain the crystal structure of consecutive planes of atoms. This simple concept can be best explained in fig. 1.7.

1. The X-rays should be regularly reflected by the ions in any one plane.
2. The reflected rays from consecutive planes should interfere constructively.

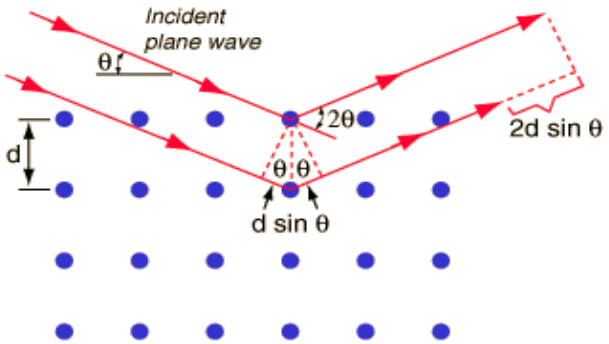

Fig. 1.7 Bragg's concept

When X-rays are scattered from a crystal lattice then the peaks of scattered intensity are observed which correspond to the following two conditions:

- The angle of incidence should be equal to angle of scattering.
- The path length difference is always equal to an integer number of wavelengths.

$$n\lambda = 2d\sin\theta$$

Eqn. 1.1 Bragg's Equation

Where,

n is an integer

λ is the wavelength of X-rays

d is the spacing between the planes of atoms

θ is the angle of incidence relative to the normal of the plane of atoms

It is a mathematical form of Bragg's law (Eqn. 1.1). When the law is fulfilled the reflected beams are in phase and give constructive interference. At angle of incidence where reflected beams are out of phase destructive interference results, causing cancellation of the waves. Crystals contain thousands of planes and the law imposes a strict condition on the angles accountable for the reflections.
This equation allows each observed diffracted X-ray beam, known as reflection to be uniquely labelled with the three h, k, and l indices and for its net scatter in angle to be calculated from the unit cell geometry. The relationship between d spacing, unit-cell dimensions and Miller indices explains the idea of a crystal system.

1.5.6. Symmetry

Molecules can have their symmetry described as point group symmetry. It explains actions such as rotations and mirror plane reflections that can be performed upon a molecule. To perform these actions, it is essential that the symmetry operator produce a representation of the molecule that is identical from the original. However, crystals have effectively repeating structures so they may also possess space symmetry, which involves a combination of molecular point symmetry elements with incremental translational steps through the structure.

The space symmetry elements, screw axes and glide planes, are derived from their respective point symmetry elements, rotation axes and mirror planes by adding a translational step in between each operation of rotation.

The presence of symmetry elements in a crystal structure imposes restrictions on the geometry of the lattice and the unit cell, .i.e. a, b, c and α, β, γ.

These are related to how the units pack together. There are a number of ways of packing three dimensional objects in space with no gaps between them. On this basis, the crystal symmetry can be divided into seven crystal systems as shown in table 1.1.

1.5.7. The intensities of diffracted X-rays

The intensities of X-rays are critical in the determination of unknown crystal structures. There are two numerical values linked with each reflection in the diffraction pattern.
These are:

1. amplitude[F] ,related to the intensity, I, of the wave function:

$$I \propto [F]^2$$

2. phase

By summing each individual scattered beam from each atom in the unit cell, the final amplitude and phase can be calculated. This calculated amplitude is known as structure factor, F_{hkl} for hkl reflection. The structure factor is defined by the phase,ϕ**,** and amplitude [F] of the wave and is calculated using the scattering power of the atoms, f_i and their positions x, y, z, . The formation of an image of the atomic arrangement from the diffraction pattern is carried out by Fourier transformation. The diffraction pattern is the Fourier transformation of the electron density and electron density is itself the Fourier transformation of the diffraction pattern. In this relationship, the diffraction can be referred to as forward Fourier transformation, and the calculation of electron densities from the diffraction pattern is referred as the reverse Fourier transformation.

1.5.8. Phase problem

Both the amplitude, [F] and the phase, ϕ of the waves, are required for Fourier transformation. However the diffraction pattern only directly contains information about [F] and not ϕ i.e. during the forward Fourier transformation all phase information has been lost. This is known as the phase problem.

1.5.9. Structure Solution and the Phase Problem

There are two methods that we use to obtain initial information about the phases of the structure factors. These are:

1. Heavy atom method (Patterson Method – ignore the phase problem)
2. Direct methods (statistical methods and reasonable assumptions)

Heavy atom method (Patterson Methods – ignore the phase problem)

Patterson methods are normally applied to solve the structures only when the crystal contains heavy atoms or a significant fraction of the structure is already known. The initial information provided by the identification of the correct atomic position of the heavy atoms and some of the other atoms helps to calculate the structure factors including their phases. Then, this initial model can be refined to determine the rest of the electron density and thus solve the crystal structure. The interpretation of the Patterson function[13,14] is given in eqn.1.2:

$$P(uvw) = (1/V) \sum_h \sum_k \sum_l \{|F(hkl)|^2 \cos[2\pi(hu + kv + lw)]\}$$

Eqn.1.2 Mathematical form of Patterson function

This relation reveals interatomic vectors within the unit cell. The intensity of each peak is proportional to the product of the atomic numbers of the two atoms to which the vector refers. This makes Patterson functions particularly effective for the identification of the position of heavy atoms. It gives a large value in position which corresponds to interatomic vectors.

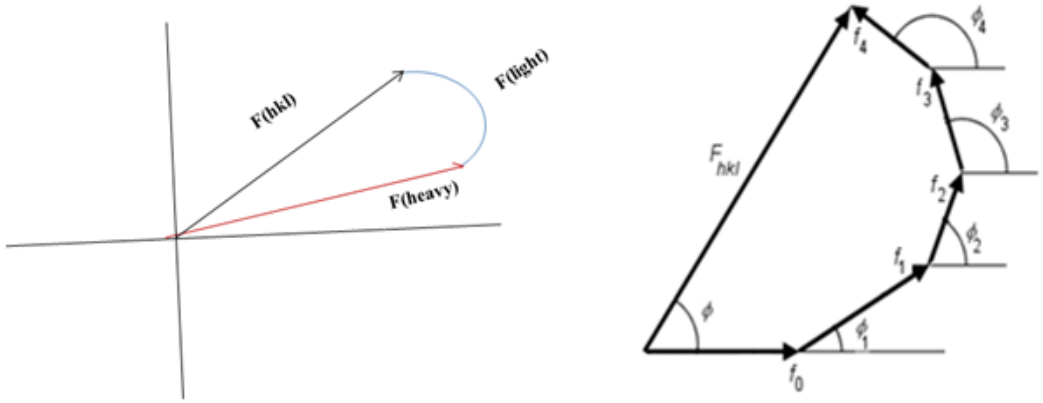

Fig. 1.9 Heavy atom method

The resultant of heavy atoms in two different forms

This Patterson map is composed of a superposition of distances A---B between pairs of atoms A B projected so that A is always on the origin of the map. The peak intensity is proportional to $Z_A \times Z_B$. The figure 1.9 shows how the structure factor is derived by vector addition of the scattered waves from the different contributing atoms in the unit cell. It is clear that the total phase angle φ will be small, and that the net phase of the structure factor differs very little from that of the heavy atom component alone.

If the positions of known heavy atoms can be determined in this way, then the Patterson map, which describes interatomic vectors, allows nearby peaks to be assigned to other atoms in accordance with expected molecular geometry. These are then used in calculating phase angles for the next approximate electron density map.

A practical limitation is that a heavy atom that dominates the vector distribution is also likely to dominate the X-ray scattering as a whole, and overwhelm diffraction peaks from less strongly scattering species. Because of the development of computers, the direct method is now the most useful technique for solving the phase problem.

Patterson methods for structure solution can be summarized as:

- It is used to calculate the Patterson function: P(uvw).
- It is used to solve for possible Heavy atom position(s).
- The position and the electron density are used to calculate an approximate phase angle $\alpha_{(hkl)}$ for each reflection. Then $\rho(xyz)$ is calculated and plotted.
- It infers the electron density map in a chemically practical way.

Direct Methods – statistical methods and reasonable assumptions

This method is used to solve the phase problem of small molecules. It is a statistical method to solve the phase problem that depends on the following assumption:

- The electron density in the unit cell can never be less than zero.
- The atoms are discrete entities.

The implication of the first requirement is that the phases used for the Fourier transformation of the structure factors must produce a result that has the least amount of "negative" electron density.

Direct methods[13,14] employ phase relationships that are probably true to generate an initial set of phases/electron density map. Structure factors with large amplitudes correspond to regions having large amounts of electron density and are thus most important for the determination of phase information. Direct Method uses "normalized" structure factors *E(hkl)* instead of *F(hkl)* to allow the statistical methods to work as given in eqn.1.3.

$$E(hkl)^2 = F(hkl)^2 / (e \Sigma f_j^2)$$ ----------**Eqn.1.3. A statistical relation for direct method**

Where e is an integer depending on *(hkl)* that corrects for the angular dependence of scattering intensity for the given reflection (i.e. the amplitude of *E(hkl)* does not depend on θ).

All structures in this project were solved by using direct methods. It estimates the initial phases and expanding phases using a triple relation. A number of initial phases are tested and selected by this method. This leads to probabilistic relationships such as: if F(hkl) and F(2h,2k,2l) are both large then their phase must be the same. Once the phase is known, approximate atomic positions are known.

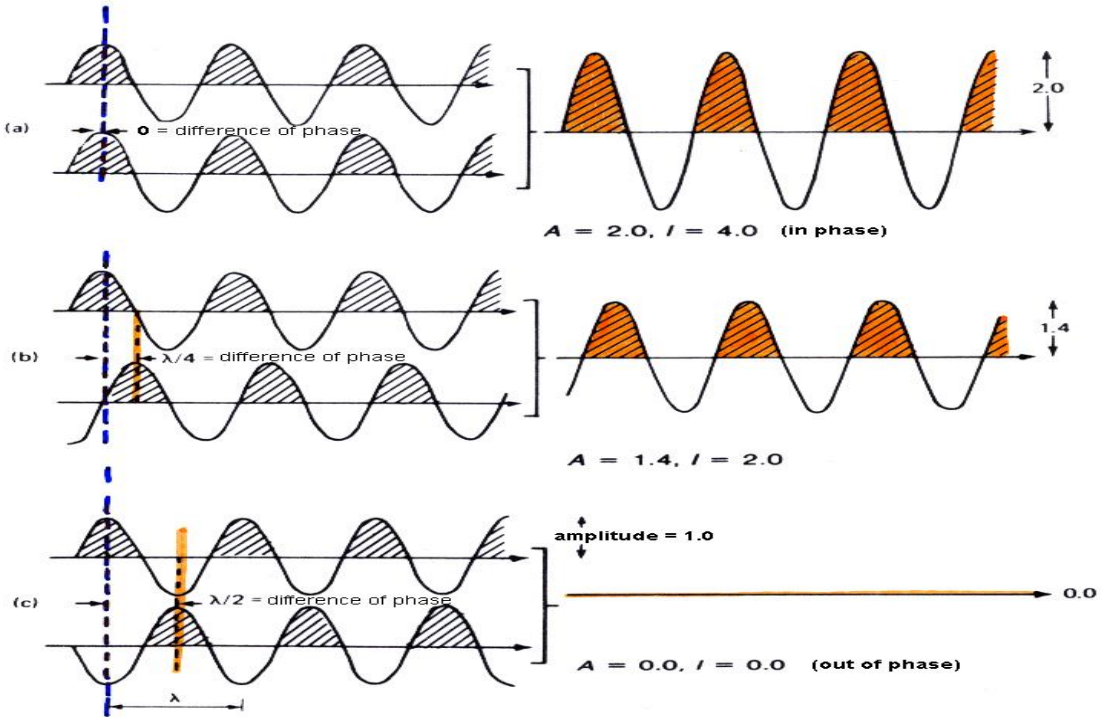

Fig. 1.10 the resultant of the scattered waves

A = resultant amplitude; I = resultant intensity (~ A^2)

(a) total in phase effect (b) partial effect of phase (c) out of phase effect

Usually waves and scattered waves, in this method, interact with each other, producing a single diffracted beam in each direction of space, so that, depending on the phase differences among the individual scattered waves, they add or subtract to give the resultants as shown above in fig. 1.10.

In short direct methods for structure solution can be summarized as:

1. This method is used to identify the strongest reflections.

2. It assumes the phases of the reflections and determines the appropriate phase relationships.

3. These assumptions are used to calculate an approximate phase angle $\alpha_{(hkl)}$ for each reflection.

4. These approximate $\alpha_{(hkl)}$ values are used to calculate $\rho(xyz)$ and plotted.

5. It interprets the electron density map in a chemically sensible way.

1.5.10. Refining and completing structure

After solving the phase problem, some atomic positions will be known. To find all the atomic positions an electron density map refining the structure SHELXL97 is generally used, usually in a Gui, such as WinGX, which also support a site of other useful crystallographic packages.

SHELXL97 requires two input files to run the programme:

1) The .ins instruction file
2) The .hkl reflection data file

The .ins takes the format as shown below.(Fig. 1.11)

It operates on a certain commands for the refining of a compound. Some important commands are as given below:

- TITL- To know title and space group structure
- CELL- The unit cell dimensions and wavelength of X-ray used
- ZERRn- Z value, n number of formula unit per cell, cell order
- LATT- lattice type information
- SYMM- symmetry operation to generate the unit cell

- SFAC- scattering factor of the given element
- UNIT- kind and number of atoms in unit cell
- MERG- merg the reflections
- OMIT- supressed bad reflections. It also contains atomic information such as fractional atomic positions

The .hkl file contains each reflections recorded, along with its hkl indices and its relative intensity.

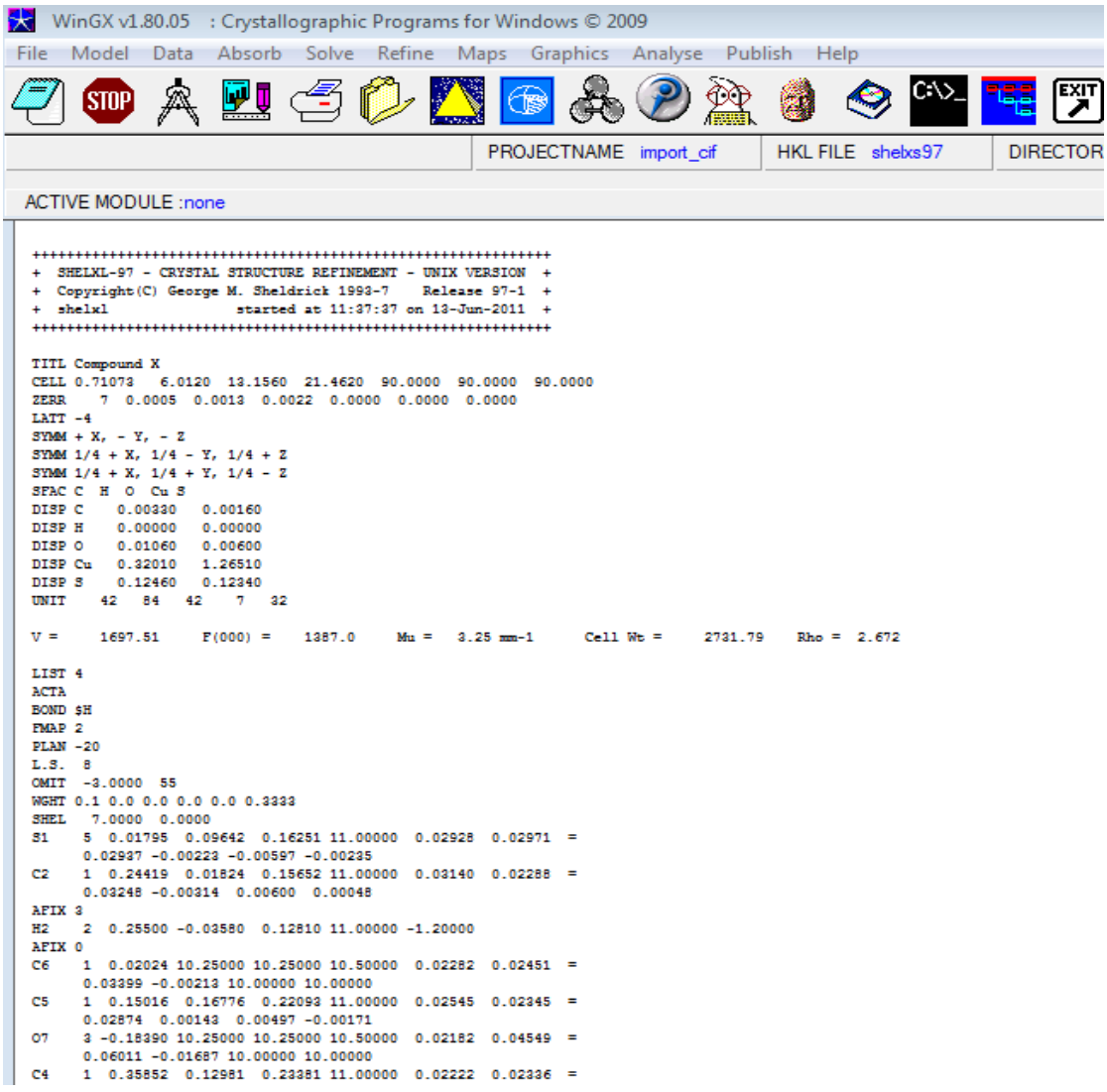

Fig. 1.11 **Screen grab of the SHELXL .ins file**

1.5.11. R-factors

The diffraction pattern that would occur if the proposed structure is correct is calculated, generating a set of calculated structure factor F. Comparison of calculated and observed |F| values provides a measure of the accuracy of the proposed atomic parameters and is assessed by a residual factor or R-factor. $R = \Sigma_{All\ hkl} |(|F_{obs}| - |F_{calc}|)|/\Sigma|F_{obs}|$

wR is similar to R except F_{obs} have been weighted according to accuracy. Other types of R factors use F^2 but they are all low for good agreement between observed and calculated structure factors. Adjusting x, y and z, so that R is minimized, will produce the optimal molecular geometry.

The SHELXL97 programme use F^2 values and includes a statistical weighting scheme for each reflection, resulting in a meaningful R factor. SHELXL97 will then label the atoms found according to their electron densities. The hydrogen atoms are rarely found at this stage. It is due to their low number of electrons. Once heavy atoms are found hydrogen atoms can be found from difference Fourier maps or constrained to chemically reasonable positions.

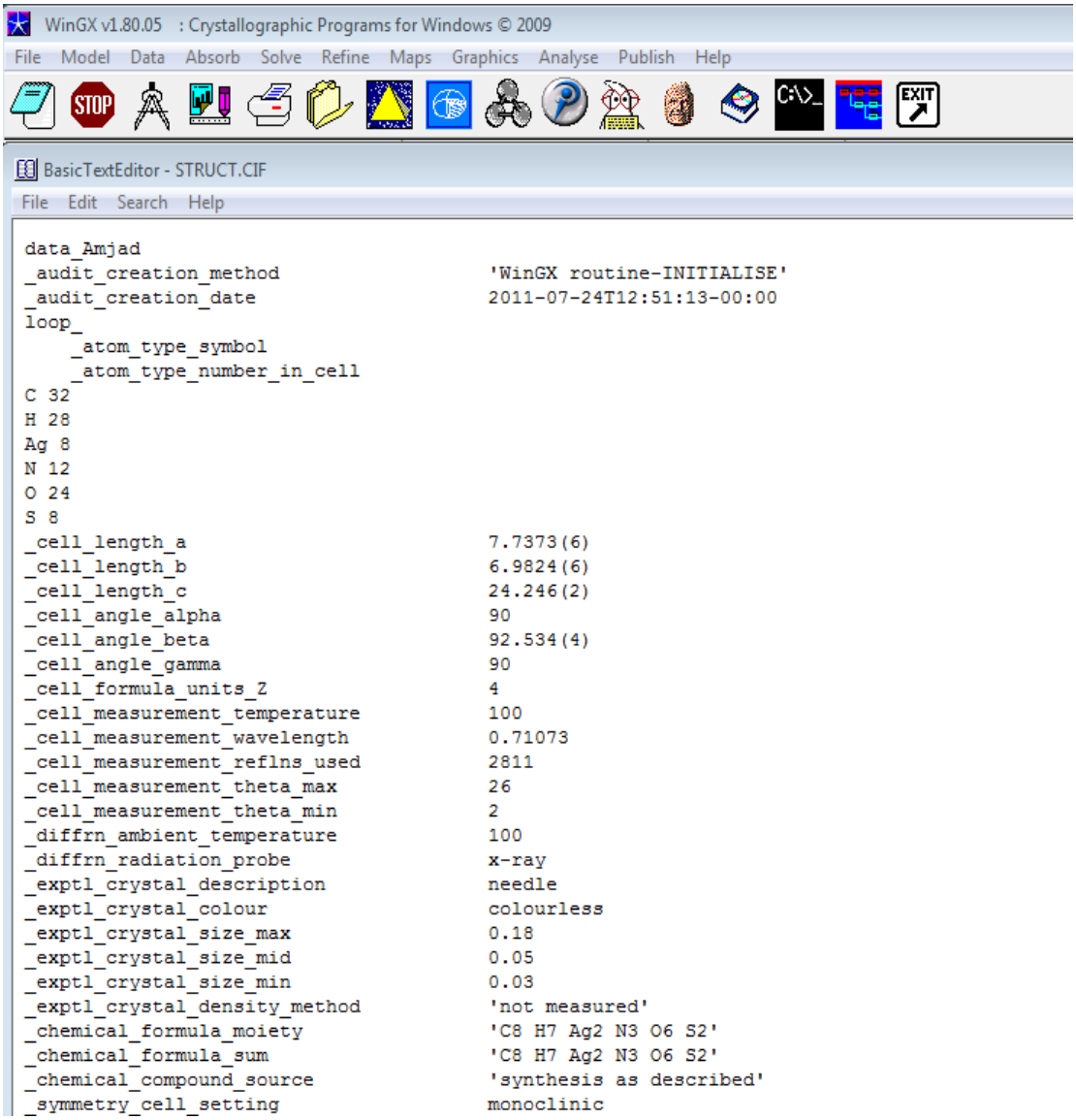

Fig. 1.12 **Screen grab of the SHELXL-97 output window**

Refining the structure involves varying the numerical parameters describing the structure to produce the best agreement between the calculated and the observed diffraction pattern. However, the process is non-trivial for refinement of crystal structure because:

1. There are many variables
2. Fourier transform is far from linear

This is why refinement can only be conducted once a reasonable model structure has been obtained and each least squares cycle is only approximate. Hence many least squares cycles are needed before convergence has been achieved.

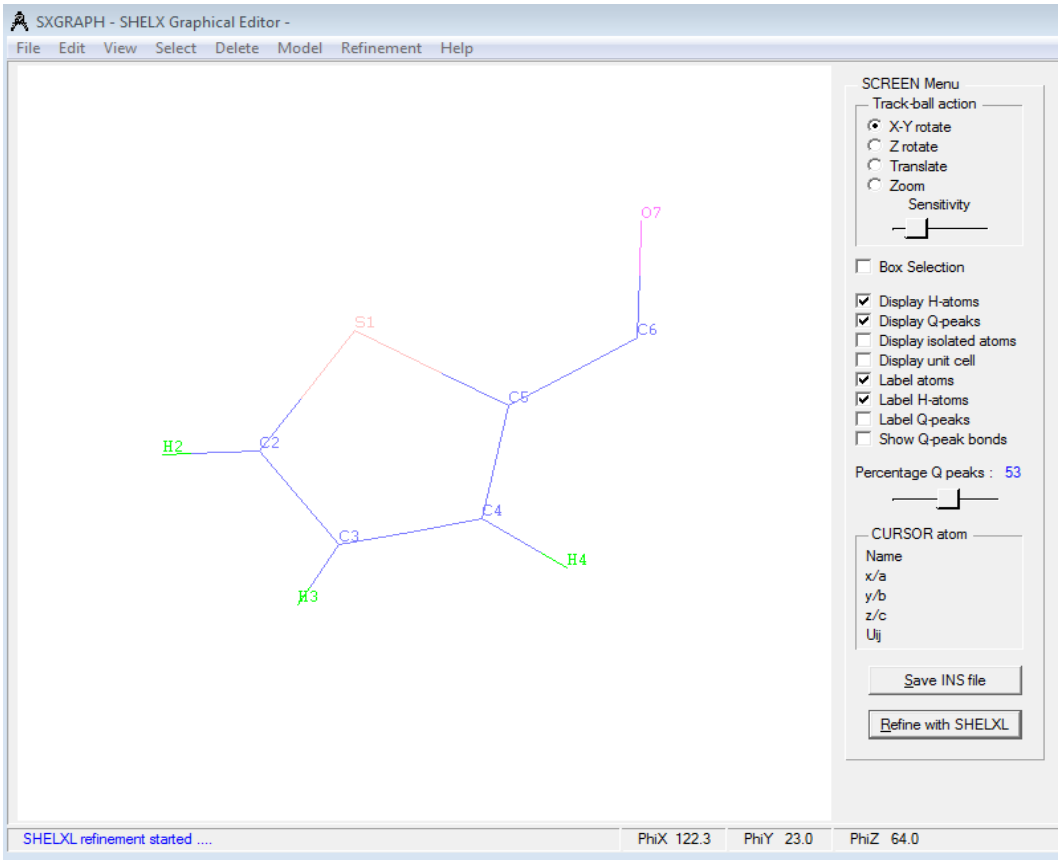

Fig. 1.13 Structure obtained using SHELX graphic editor

In order to get the position of hydrogen, the refinement of non-hydrogen atoms must be conducted anisotropically. This is done by allowing more than one displacement parameter per atom in the model structure, allowing each

atom to vibrate by different amounts in different anisotropic vibration directions. SHELXL is prompted to do this by inserting the ANIS command into the .ins file and re-running the refinement process. The least squares refinement process modifies the terms providing the position and vibrations of the atoms. For each isotropic atom there are three co-ordinates, x, y, z, and a displacement parameter, U. this can be interpreted as an isotropic mean-squared amplitude of vibration of the atoms, and for each an isotropic atom x, y, z, and 6U parameters.

1.5.12. Location of atoms in the unit-cell

After solving the structure using either Heavy atom or Direct methods it is then possible to produce a Fourier Map of the electron density $\rho(xyz)$ within the unit-cell.

Molecular graphics packages are then used to display the results in the form of molecules on the computer screen. The crystallographer is able to interact at this stage to name atoms and remove any weak peaks from the atom list.

1.6. Graphics

Several types of computer graphics are used when working on a crystal structure.

1. Stick drawing or ball and stick which are simple and uncluttered
2. Space filling. Atoms are drawn with Van der Waals radii. It is useful for trying to visualise if a reaction centre is sterically restricted.
3. Vibrational ellipsoids (ORTEP) drawing. Shows if correct atom assignment has been made and which part of the molecule is able to move within the crystal structure. Ellipsoids become smaller as the temperature is

reduced. Can be helpful in understanding disorder, where an atom partially occupies more than one site within the unit cell.

4. Packing. Several molecules are drawn, usually with unit-cell. H-bonding can be highlighted.

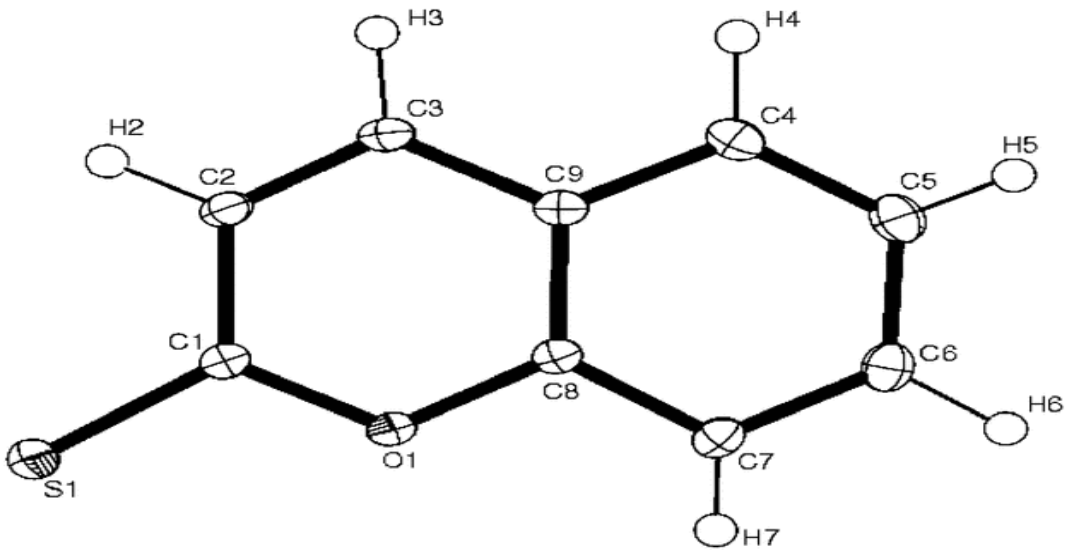

Fig. 1.14 ORTEP diagram of 2-thiocoumarin

An ORTEP structure of 2-thiocoumarin[16] is shown in fig.1.14 is showing how peripheral atoms vibrate more than core. Hydrogen atoms are typically drawn with the same small vibration for clarity.

1.7. Single Crystal X-ray Diffraction for Structure Determination

There are certain steps involved for structure determination of a compound. All these steps are interlinked step by step:

1.7.1. Growing of Crystals.

Some materials readily form crystals. The crystals can appear as a solution cools or through evaporation of the solvent. Sometimes this does not happen and the solid has to be re-dissolved and the above processes repeated. If crystals still do not form the vapour diffusion method has proved to be particularly successful. (Fig. 1.15)

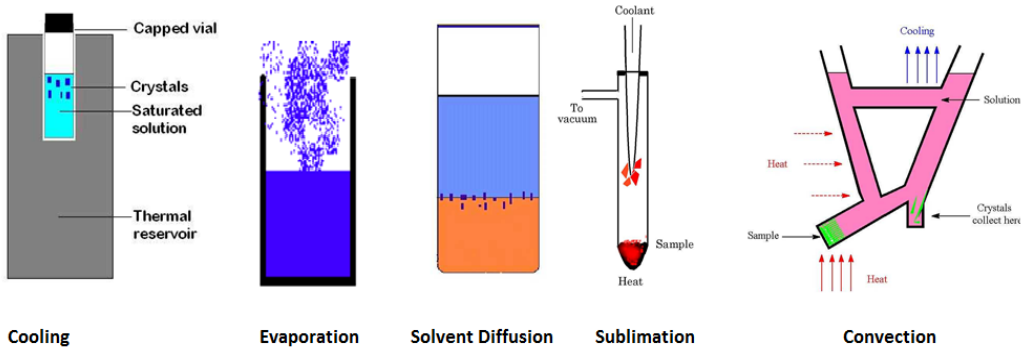

Fig.1.15 Growing of crystals

1.7.2. Selection of a suitable crystal

A polarizing microscope is used to select a suitable crystal(0.25x0.25x0.25 mm^3). It must be a single crystal as shown in fig.1.16. The crystals are immersed in an insert oil to protect them from the atmosphere. Cracks or other imperfections in the crystal stand out when viewed between crossed polarizers.

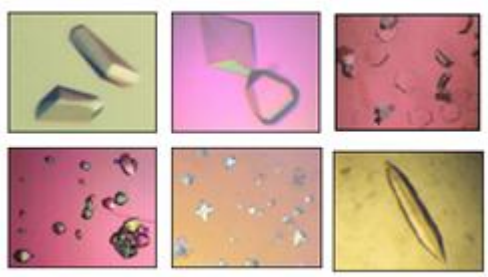

Fig.1.16 Selection of crystal

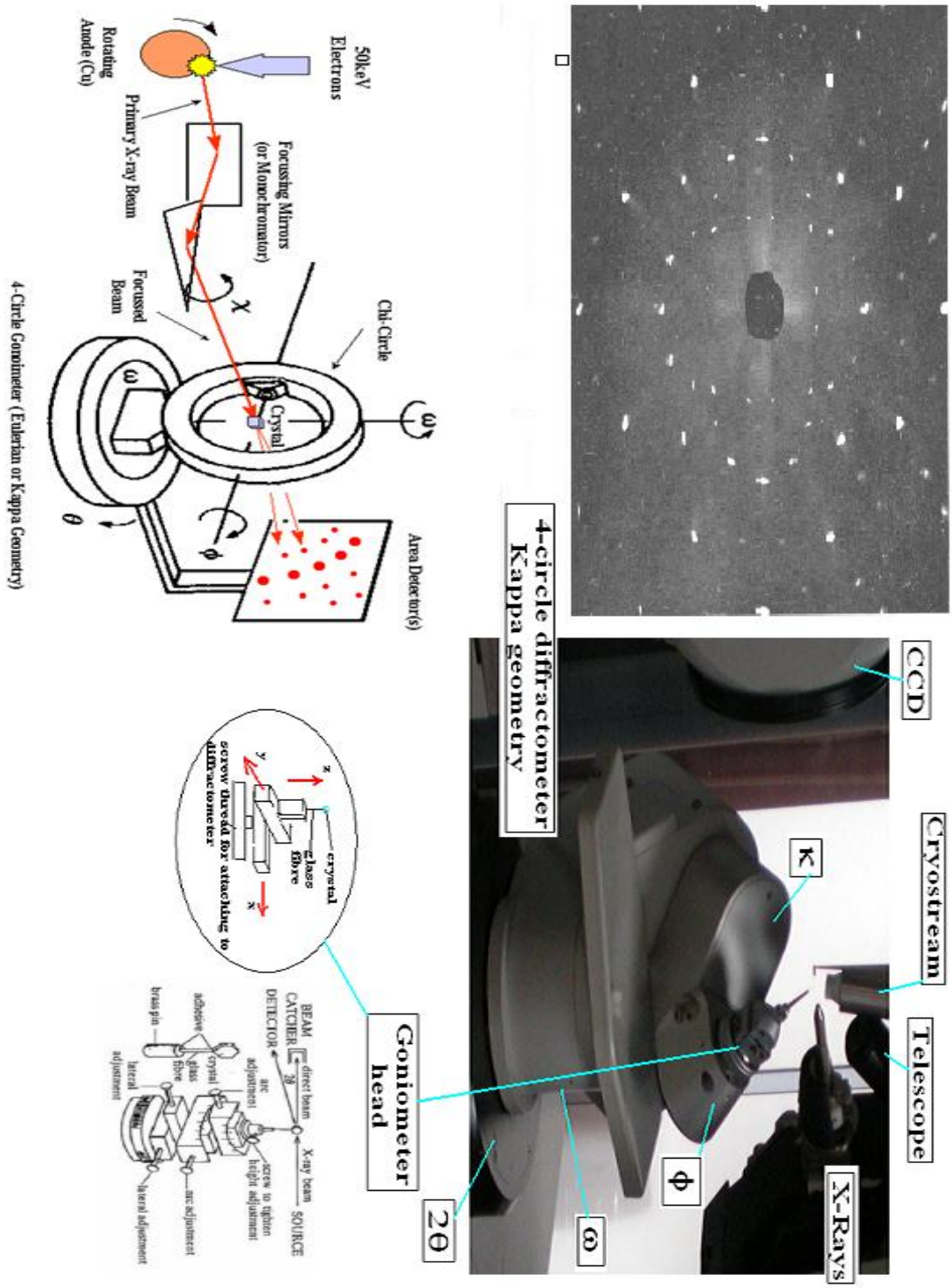

Fig. 1.17 Kappa geometry

1.7.3. Mounting the crystal on the diffractometer.

The selected crystal is placed on the tip of a glass fiber and mounted on an adjustable goniometer head in the middle of the diffractometer as shown in fig.1.18. The crystal is cooled by a stream of nitrogen gas (100 K), which protects the crystal from X-ray damage and also freezes the oil to attach the crystal to the fiber. Centre the crystal using the built in telescope and the x,y,z adjustments on the goniometer head. The diffractometer has been set so that the telescope crosswire coincides with the centre of the diffractometer.

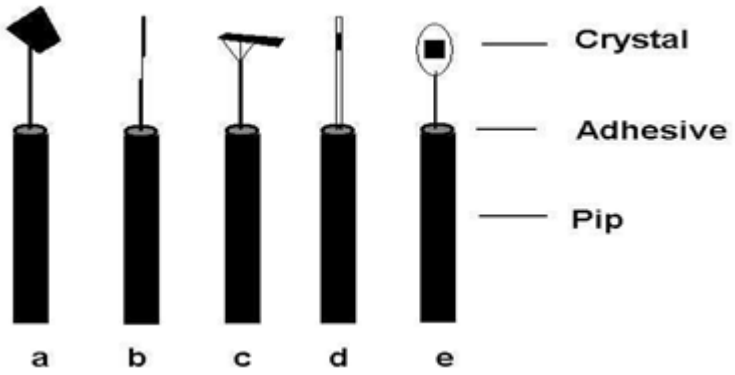

Fig.1.18 Mounting of crystal on fibre

a) on a glass fibre b) on a two stage fibre c) a fibre top with several lengths of glass wool d) within a capillary tube d) in a solvent loop

1.7.4. Unit-cell determination.

Use the CCD detector to record ten diffraction images at various crystal angles. Process the images to determine the reflection angles and hence determine the unit-cell dimensions and crystal class.

1.7.5. Measure a full set of reflections (h,k,l, Intensity)

Number of reflections depends on unit-cell dimensions and crystal system. More reflections are needed for large unit-cells and also low symmetry crystal systems.

1.7.6. Perform corrections

The raw intensity data has to be corrected for various physical effects associated with the mode of data collection

$$\text{Corrected intensity} = F^2(hkl) = I(hkl)/[(Lp) \times (Dec) \times (Abs)]$$

The Lorentz factor, L, is related to the length of time a reflection is in its diffracting position. It depends on the geometry of the diffractometer and hence method of data collection. The polarization factor, p, allows for partial polarization of the X-ray beam when it is reflected off the crystal.

Both effects are dependent on θ and a correction is easily calculated.

1.7.7. Assigning the space group.

Examine the $F^2(hkl)$ list to see if there are any systematic absences. Data collection and processing is completed at this step. Perform statistical tests on reflection intensities to detect the presence of an inversion centre. Use this information to determine the space group.

1.8. Kinds of X-ray diffraction techniques

X-ray diffraction techniques can be operated in two different ways depending upon the kind of the solids to be analysed. These are given below:

- Single crystal X-ray diffraction
- X-ray powder diffraction

1.8.1. Single crystal X-ray diffraction

The single crystal sample is a perfect (all unit cells aligned in a perfect extended pattern) crystal with a cross section of about 0.3 mm. The single crystal diffractometer and associated computer package is used mainly to elucidate the molecular structure of novel compounds, either natural products or man-made molecules.

Selection and mounting of a single crystal for X-ray diffraction

Crystals of the compound were selected by transferring onto a clean microscope. An inert, fluorinated oil (Fomblin) was used to cover the crystals and allow easy manipulation. The selection of a single crystal was crucial to avoid twinning errors. To this end, proposed crystals were viewed under cross polarised light. A single crystal will extinguish entirely at the same time, whereas if the proposed crystal is actually two crystals overlapping they will extinguish at the different times due to slight difference in orientation. Once the crystal of suitable size is selected it was transferred onto a thin (ca 0.04mm in diameter) glass fibre, supported by fomblin oil. The crystal can be mounted on the fibre in different ways as in fig.1.18. The fibre

and crystal then quickly transferred onto the goniometer head, where the stream of gaseous nitrogen, which cooled the sample to facilitate low temperature investigation, froze the crystal to the fibre, preventing slippage. The crystal was then centred in the X-ray beam by subtle adjustments of the goniometer head while observing the crystal via a video microscope feed which had crosshairs superimposed over the image.

The crystal suitability for the diffraction experiment was then tested by taking one "plate" (i.e. collect the diffraction pattern of the crystal for a small oscillation of the goniometer head).For the crystal to be a good diffractor, a series of widely spaced, sharply define spots must be recorded by the CCD.

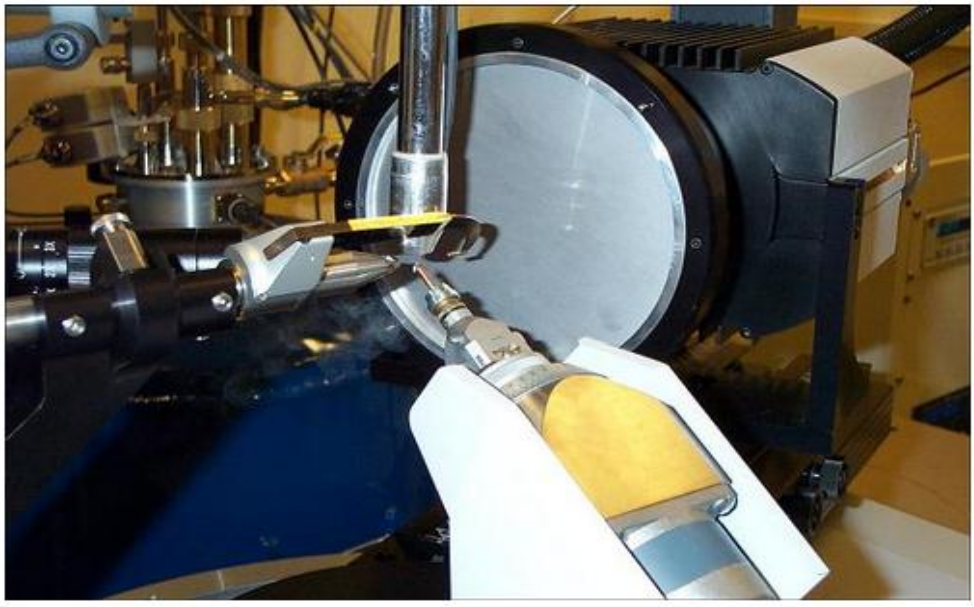

Fig.1.19 X-ray diffractometer

showing the goniometer head, collimator and Cryostream nozzle.

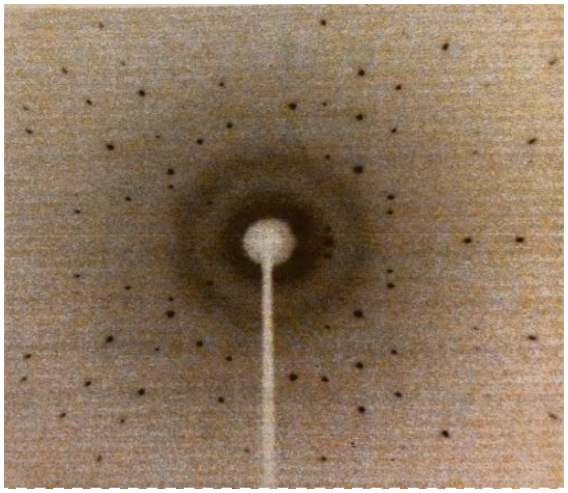

Fig. 1.20 Image captured by the CCD detector of a well diffracting crystal

An example of the sort of image a well diffracting crystal would generate on the CCD is given in fig. 1.20. The central part of the picture is dominated by the beam stop. This is to stop the most intense part of the x-ray beam from saturating the rest of the "plate", and making scaling the relative intensities of true reflections easier. The relative intensities of the different reflections can be seen as well. If the crystal is a very poor diffractor or amorphous a data set suitable for structure determination cannot be collected.

Using the program SUPERGUI, the machine is instructed to collect 10 "plates" to determine the unit cell. Once this is complete, a check of the relevant database using the acquired unit cell data was performed to check that the structure had not been solved before. If none of the possible database structures matches (by knowledge of the reactants used) then a full structure determination was performed.

1.8.1.1 Applications of Single Crystal X-ray Diffraction

Single-crystal X-ray diffraction is normally used for accurate determination of a unit cell like cell dimensions, positions of atoms within the crystal lattice. Bond angles and bond length are directly linked to the atomic positions. The crystal structure of a

compound is a distinct property that is the basis for understanding many of the properties of compounds.

Some of the applications[16] of single-crystal X-ray diffraction are given below:

- It is used for the identification of new materials.
- This technique is helpful to determine certain parameters like unit cell, bond lengths, bond angles and site ordering.
- Cation and anion coordination can be characterised by following this technique
- It is used to understand the variations in crystal lattice.
- Single-crystal X-ray diffraction is used to determine structures of high pressure and/or temperature phases in specialized chamber.
- It is used for the determination of crystal-chemical vs. environmental control on mineral chemistry.
- With the help of this technique powder patterns can be derived by using certain special cameras

Advantages:

- There is no obligation of individual standards
- It is purely non-destructive technique
- Crystal structure can be characterized fully i.e. unit cell dimensions, bond lengths, bond angles, site-ordering facts etc.

Disadvantages:

- Sample must have a single crystal between 50-250 microns in size
- Optically clear sample(crystal) is required for characterisation
- It is very difficult to handle the twinned samples (crystal).
- Generally it requires 24 to 72 hours for data collection.

1.8.2. X-ray Powder diffraction

Powder diffraction is mainly used for “finger print identification” of various solid materials, e.g. asbestos, quartz. Where it is important to have a sample with a smooth plane surface. If possible, we normally grind the sample down to particles of about 0.002 mm to 0.005 mm cross section. The ideal sample is homogeneous and the crystallites are randomly oriented. The sample is pressed into a sample holder so that we have a smooth flat surface. There is no need to move the sample in a powder diffractometer as shown in fig.1.21 &1.22 because, statistically, some crystallites will be orientated correctly for every Bragg crystal plane. A single radial scan, as illustrated, provides all necessary information.

Fig. 1.22 Bruker D5005 Powder diffractometer

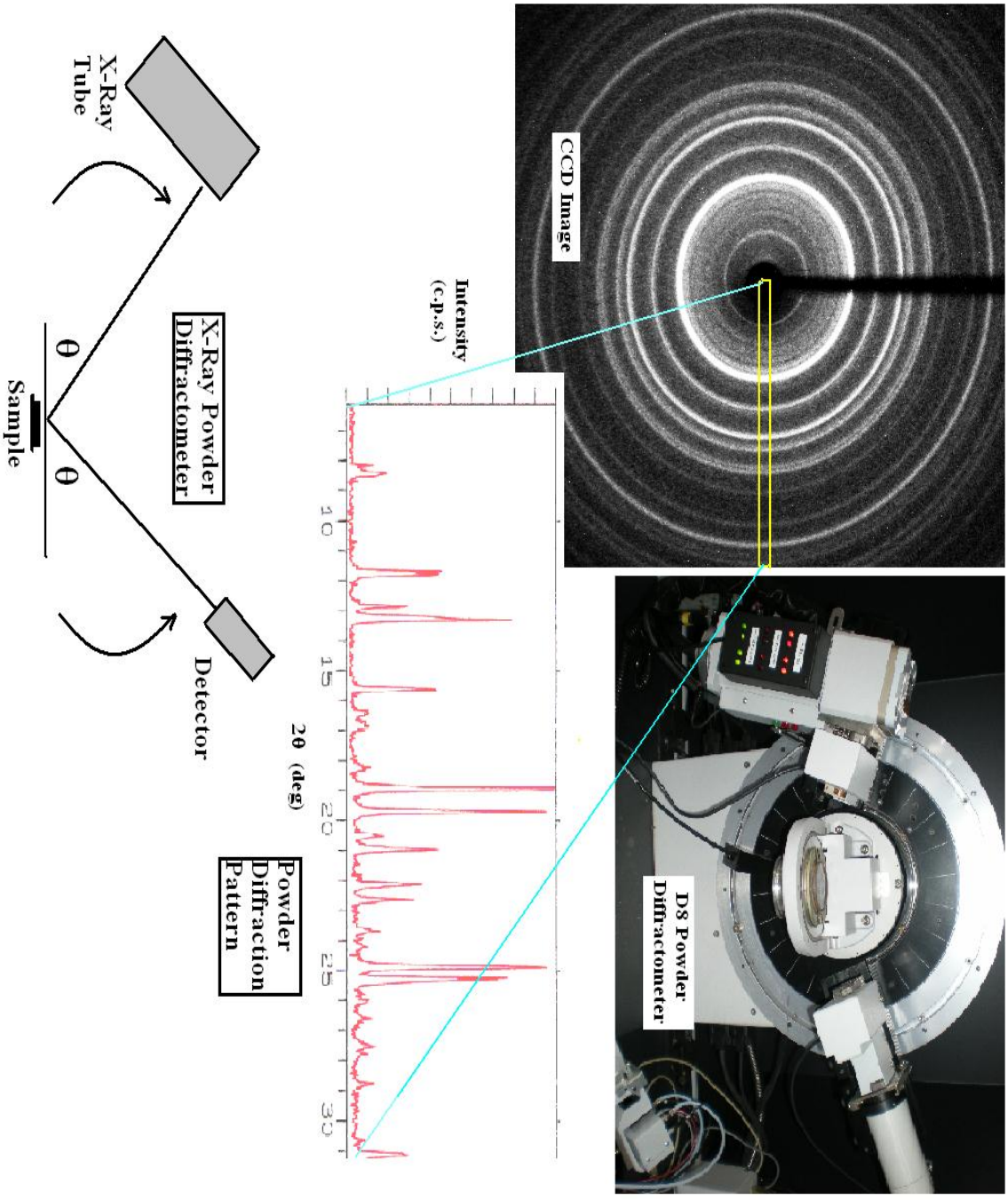

Fig. 1.21 Powder diffractometer/Pattern/CCD Image

This is achieved by moving the X-ray source through θ accompanied by an identical detector movement. The diffraction pattern is a trace of X-ray intensity vs. 2θ and consists of a series of peaks, corresponding to Bragg reflections.

1.8.2.1. Applications of Powder Diffraction

X-ray powder diffraction is most widely used as a finger print of unknown materials. Determination of unknown solids is critical to studies in geology, environmental science, material science, engineering and biology and forensic science.

The main applications[16] are:

- It is widely used for the characterization of crystalline materials
- To find out stress and strain in metal and fine-grained mineral
- Unit cell dimensions and crystal structures can be determined
- XRD is used for quantitative analysis and measure the purity of sample
- Super lattices in multi-layered epitaxial structures can be measured
- X-ray reflectivity measurements are used to determine the breadth, density and coarseness of the film.

Advantages of X-ray Powder Diffraction (XRD)

- It is widely used to get finger prints of complexes in short times(< 20 min)
- It is a powerful tool for identification of an unknown mineral
- It can be operated with small amount of sample
- These units are commonly available

Disadvantages of X-ray Powder Diffraction (XRD)

- It is best to use for homogeneous and single phase material
- A routine search cannot be carried out without the availability of a standard reference file (d-spacing, *hkl*s)
- The sample to be analysed must be pulverized into fine powder
- Results for mixed materials can be difficult to interpret because of peak overlap

- It is difficult to operate for unit cell determinations, indexing of patterns for non-isometric crystal systems

1.9. Types of radiation used for crystallography

The following "radiations" have the correct wavelength to be diffracted by molecules and crystals but, because of their different properties, are able to highlight different aspects of the material under investigation.

Table 1.4

Types of radiation used for crystallography

"Radiation" type	Source	Scattered by	Aspect highlighted
X-rays	Sealed tube, Rotating anode or Synchrotron	Electrons	Heavy elements such as lead dominate a structure.
Neutrons	Nuclear reactor	Nuclear spin	Light elements can be seen clearly, even in presence of heavy atoms. Also magnetic properties can be discerned
Electrons	Electron gun	Nuclear charge and electrons	Scattered very easily. Good for studying very thin layers and gases but must work in vacuum

a) Neutron diffraction: Frequently used to complement X-ray methods by highlighting hydrogen locations.

b) Synchrotron: Provides very intense X-rays with a wide range of wavelengths for carrying out many types of experiments (1000 x intensity of sealed tubes).

1.10. Crystallographic Databases

Four generally available databases are used to store crystallographic information of interest to chemists:-

1) Joint Committee on Powder Diffraction Standards (JCPDS) powder diffraction file contains about 60,000 powder diffraction patterns.

2) Crystal Data Identification File (CDIF) contains unit-cell information for over 200,000 compounds, 70,000 of which aren't in the ICSD or CCDC databases.

3) Inorganic Crystal Structure Data base (ICSD) contains full structural information for over 60,000 inorganic structures.

4) Full structural information for over 300,000 organic and organometallic structures (any compound containing carbon) has been compiled at the Cambridge Crystallographic Data Centre (CCDC).

Chapter 2

X-ray Crystallographic Study of Copper(I) Complex With 3-Methylbenzothiazole-2-Thione

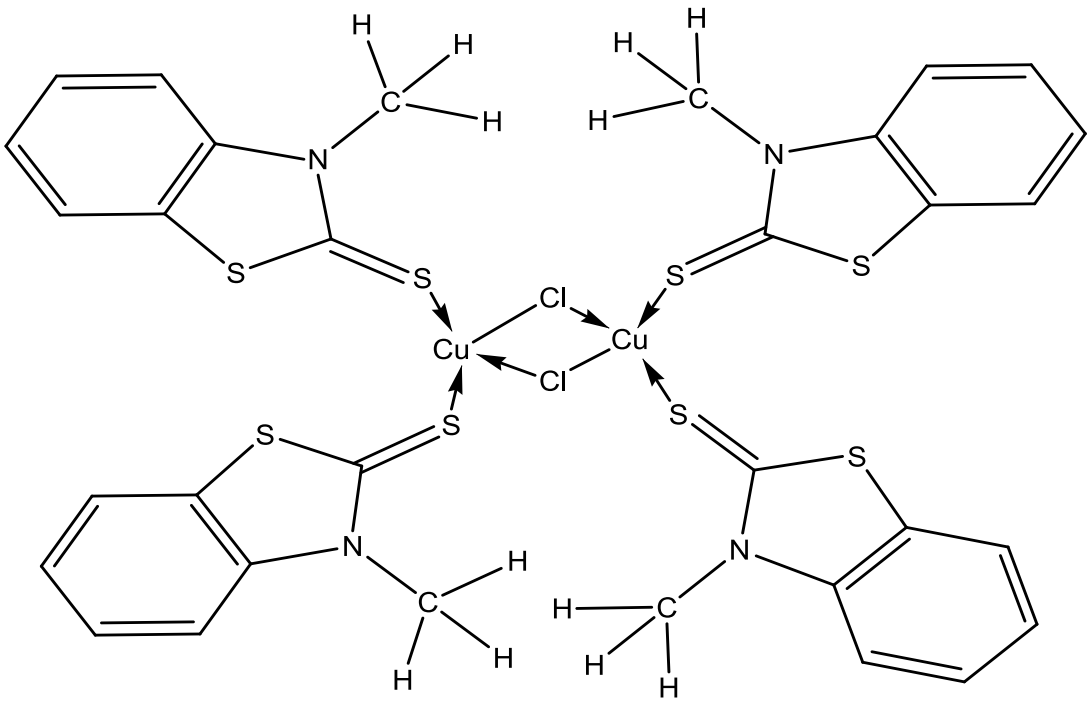

2. Introduction

A polymeric complex of copper(I) with 3-methylbenzothiazole-2-thione (mbtt), has previously been synthesized and studied[5,6]. The synthesis and crystallographic data of a novel dimmeric Cu(I)Cl complex with 3-methylbenzothiazole-2-thione (mbtt) are described in this work. This was obtained from reactions of Cu(I)Cl with 3-methylbenzothiazole-2-thione (mbtt), in methanol (dry) in a very dilute solution under mild experimental conditions. Single crystal X-ray diffraction has been used to characterise and study the compound. The coordination of mbtt with copper(I) and crystallographic properties have been studied.

2.1. Experimental

2.1.1. Chemical reagents

Originally pure copper(I)chloride is a white powder, which changes its colour to pale green slowly due to the oxidation of copper(I) to copper(II). Copper(II) was removed from the sample used in this project to produce analytical standard Cu(I)Cl as explained in the literature[17,7].

The heterocyclic compound 3-methylbenzothiazole-2-thione (mbtt) was used in its original form.

2.1.2 Preparation of reagents

A. 0.01M solution of Cu(I)Cl is prepared in methanol. The compound is partially soluble in methanol hence slightly greater amount of Cu(I)Cl is used to get solution of required concentration.

B. In the same way 0.01M solution of 3-methylbenzothiazole-2-thione (mbtt), ($C_8H_7NS_2$) is prepared.

The whole procedure is done under normal laboratory conditions.

2.2. Synthesis of $\mu_2Cl_2[Cu_2(mbtt)_4]$

To a solution of copper(I)chloride (0.025 g, 0.01M) in methanol was added a solution of 3-methylbenzothiazole-2-thione (0.025 g, 0.01M) in methanol. The Cu(I)Cl and 3-methylbenzothiazole-2-thione in 2:1 molar ratio (M:L) in methanol were left to react uninterrupted for one week . The slow evaporation of the solution at room temperature gave white prismatic crystals of the complex.
The study focused on the intriguing behaviour of copper(I)chloride with 3-methylbenzothiazole-2-thione.

2.3. Structure Determination and Refinement

A single crystal of compound was mounted on an X-ray Kappa diffractometer equipped with a graphite monochromator and Mo Kα radiation (λ = 0.71073 Å). The unit cell dimensions and intensity data were measured at 100K. The structure was solved by direct methods. Then it was refined by the full matrix least squares based on F^2 with anisotropic thermal parameters for the non-hydrogen atoms using CCD (data collection), SHELXS-97 (structure solution), SHELXL-97 (structure refinement) and WinGX (molecular graphics). A crystal structure is obtained from the data as displayed below in fig. 2.1 and in ORTEP structure by fig 2.1a. This is a unique new structure as there is no such structure available in crystal structure database.

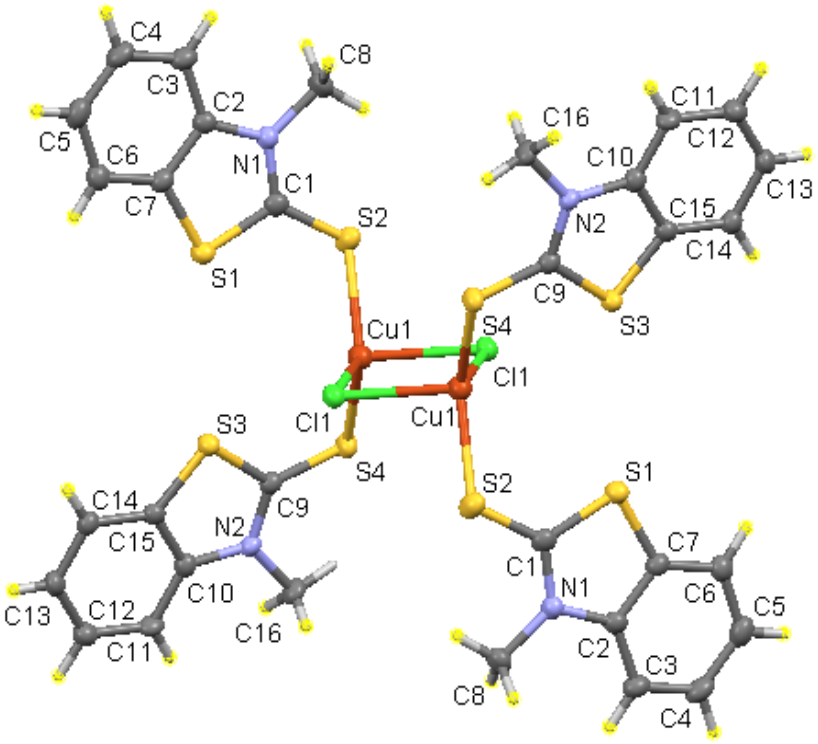

Fig. 2.1 Crystallographic structure of $\mu_2Cl_2[Cu_2(mbtt)_4]$

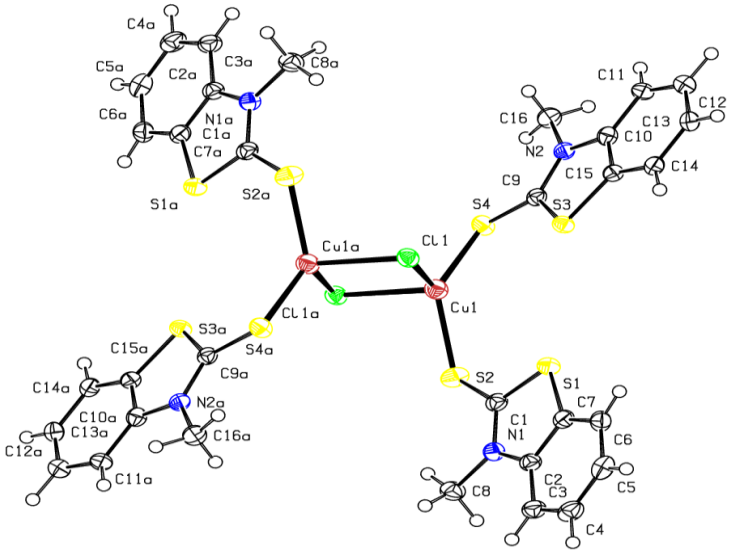

Fig. 2.1a An ORTEP structure of $\mu_2Cl_2[Cu_2(mbtt)_4]$

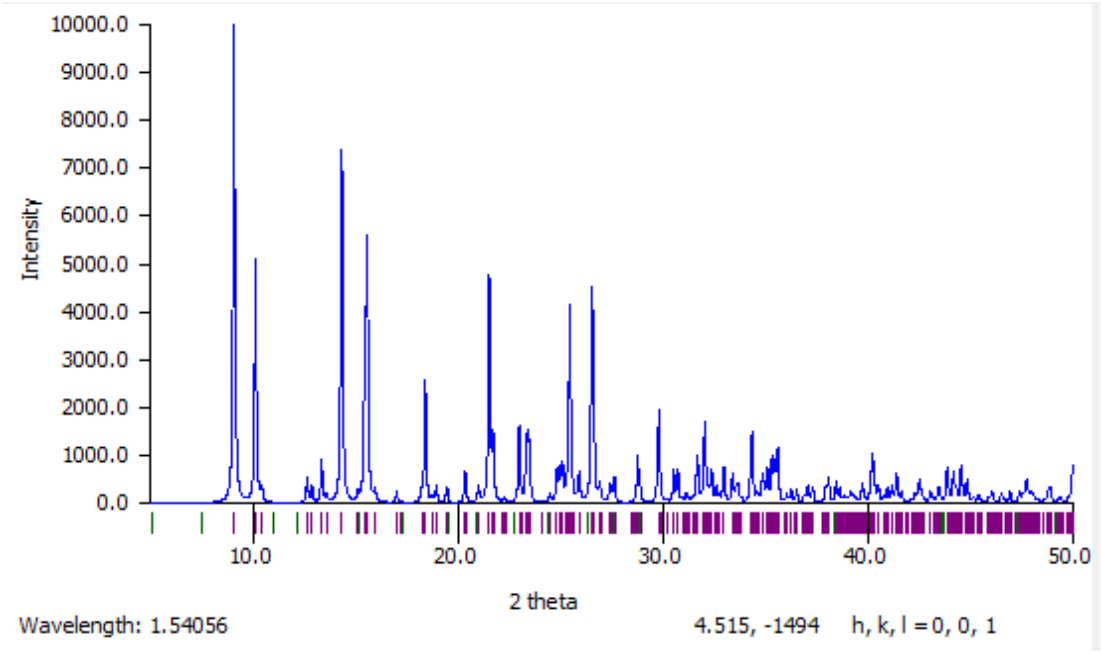

Fig. 2.1b Powder diffraction pattern of $\mu_2Cl_2[Cu_2(mbtt)_4]$ complex

The powder diffraction pattern were in the form of XY plot which covers '2θ' range on x-axis and linear count (Intensity) were along y-axis as shown in fig. 2.1b which shows peak intensity range in between 5^o-50^o.

For all non-hydrogen atoms positional and anisotropic atomic displacement parameters were refined. Hydrogen atoms were attached in static positions mounted on attached atoms with isotropic thermal parameters 1.2 times those of their carrier atoms. Criteria of a satisfactory complete analysis were the ratios of ''rms" shift to standard deviation less than 0.001 and no significant features in final difference maps. The general crystallographic data for complex is given in Table 2.1.

Table. 2.1

Crystallographic structure data of $\mu_2Cl_2[Cu_2(mbtt)_4]$

Parameters	Description	Parameters	Description
Empirical formula	$C_{16}H_{14}Cl_1Cu_1N_2S_4$	Density D_x	1.759 Mg m^{-3}
Molecular mass M_r	923.04	Cell parameters	5733 reflections
Crystal system	Monoclinic	Mo $K\alpha$ radiation, λ	0.71073 Å
Space group	$P2_1/c$	Cell reflections I	3996
Nature of crystals	Colourless, prism	Z	2
a	8.5367 (3) Å	μ	1.89 mm^{-1}
b	11.7037 (4) Å	T	150 K
c	17.5842 (7) Å	wR	0.112
β	97.316 (1)°	R	0.043
Cell volume	1742.55 (11) $Å^3$	R_{int}	0.041

Similarly crystallographic data for complex $\mu_2Cl_2[Cu_2(mbtt)_4]$ regarding bond length and bond angle with symmetry codes is given in Table 2.2 and Table 2.3 respectively.

Symmetry code: (i) -x, -y+1, -z+1.

Table 2.2

Bond angles of complex $\mu_2Cl_2[Cu_2(mbtt)_4]$

Parameter	BondAngle(Å)	Parameter	BondAngle(Å)
C1—N1—C2	115.1 (3)	C9—N2—C10	114.5 (3)
C1—N1—C8	123.5 (3)	C9—N2—C16	123.7 (3)
C2—N1—C8	121.2 (3)	C10—N2—C16	121.7 (3)
C1—S1—C7	91.48 (18)	C9—S3—C15	91.76 (17)
C1—S2—Cu1	113.96 (14)	C9—S4—Cu1	107.91(13)
Cu1—Cl1—Cu1i	77.17 (3)	S4—Cu1—S2	124.86 (4)
S2—Cu1—Cl1	117.68 (4)	S4—Cu1—Cl1	111.05 (4)
S2—Cu1—Cl1i	92.91 (4)	S4—Cu1—Cl1i	100.22 (3)
Cl1—Cu1—Cl1i	102.83 (3)	S4—Cu1—Cu1i	115.19 (4)
Cl1—Cu1—Cu1i	53.54 (3)	S2—Cu1—Cu1i	113.77 (4)
Cl1i—Cu1—Cu1i	49.29 (2)		

Table 2.3

Bond lengths of $\mu_2Cl_2[Cu_2(mbtt)_4]$

Parmeter	Bond Length(Å)	Parmeter	Bond Length(Å)
C1—N1	1.348 (5)	C9—N2	1.355 (4)
C1—S2	1.678 (4)	C9—S4	1.684 (4)
C1—S1	1.736 (4)	C9—S3	1.725 (4)
C2—N1	1.395 (5)	C10—N2	1.401 (4)
C2—C3	1.395 (5)	C10—C11	1.387 (5)
C2—C7	1.389 (5)	C10—C15	1.397 (5)
C3—C4	1.387 (6)	C11—C12	1.387 (5)
C4—C5	1.392 (6)	C12—C13	1.393 (6)
C5—C6	1.388 (6)	C13—C14	1.384 (5)
C6—C7	1.397 (5)	C14—C15	1.394 (5)
C7—S1	1.744 (4)	C15—S3	1.737 (4)
C8—N1	1.464 (5)	C16—N2	1.465 (5)
C3—H3	0.94 (5)	C11—H11	0.87 (4)
C4—H4	0.93 (4)	C12—H12	0.99 (4)
C5—H5	0.93 (5)	C13—H13	0.86 (4)
C6—H6	0.90 (5)	C14—H14	0.87 (4)
S2—Cu1	2.3066 (11)	S4—Cu1	2.3050 (10)
Cl1—Cu1	2.3611 (10)	Cu1—Cl1i	2.5052(10)

The Cu-thione has monoclinic cell with space group P21/c. The central Cu(1) atom is tetrahedrally coordinated by two chlorine atoms and two sulphur atoms. The two sulphur atoms coordinate to Cu bonded to thione groups separately and bonded Cl atoms are linked to other Cu via bridging to form 4-membered ring. The unit cell contains 4 units, which stack in a highly ordered packing along the 001 axis throughout the crystal system. The short contact view of the compound provides information about its preferred dimensions, molecular orientation and approximate linearity as shown in fig. 2.2.

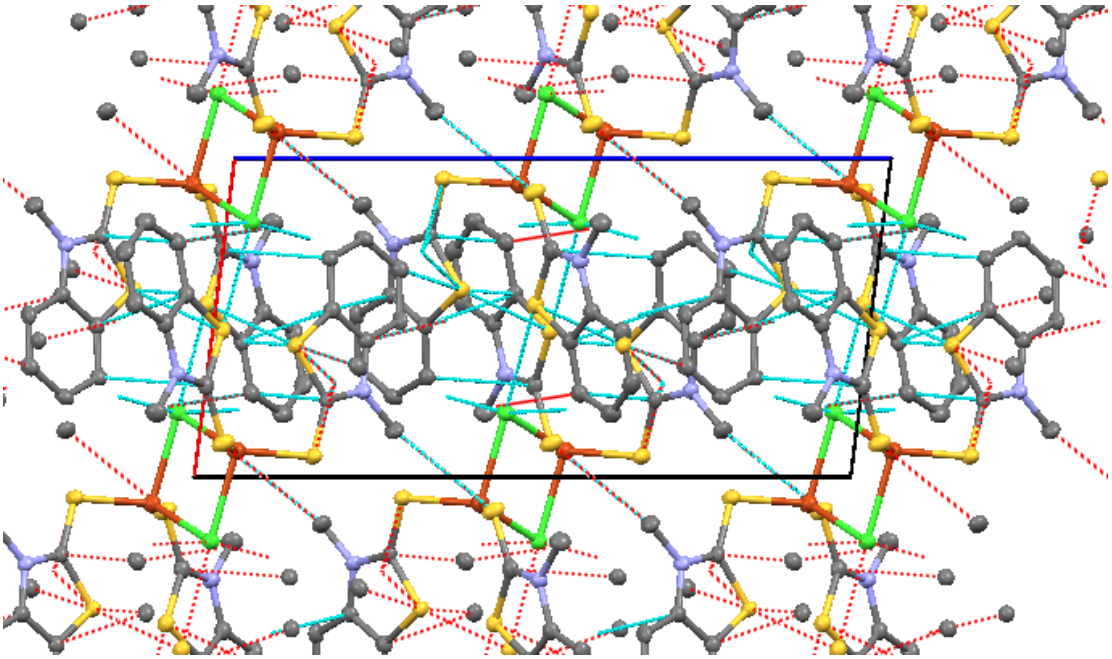

Fig. 2.2 Short contact structure of $\mu_2Cl_2[Cu_2(mbtt)_4]$

A space filling model of this structure reveals how very sterically hindered the Cu atom is, as shown in fig. 2.3. This reinforces the idea of the Cu atom playing only a structural role in the complex.

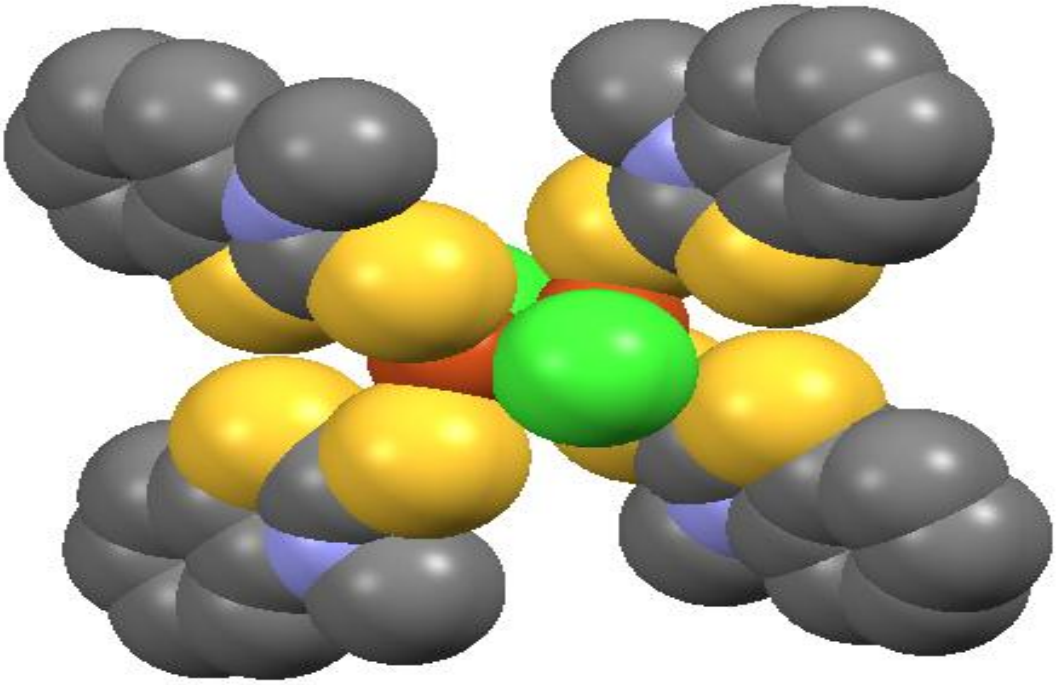

Fig. 2.3 Space filling model of complex of $\mu_2Cl_2[Cu_2(mbtt)_4]$

2.4. Results and discussion

2.4.1. Crystallographic study of $\mu_2Cl_2[Cu_2(mbtt)_4]$

This is interesting that the formation of a dimeric species is observed in which bridging takes place between Cu atoms through Cl atoms. The S atoms in four groups of the same kind of ligand as shown in fig. 2.4a, with S-bonded to SCN anions is used to bonding with Cu as shown in fig. 2.5. It shows a repeat unit of one part of a dimer along with numbering scheme. Its formation is believed to occur via the tetramer repeating unit. These repeating units are linked through Cu-S atoms, and generate dimeric complex. In the same time Cu is linked to Cl to form a bridge and a 4 membered ring is produced as shown in fig. 2.4b.

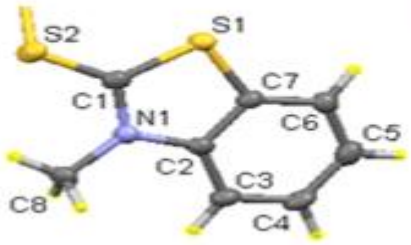

Fig. 2.4a A small unit of mbtt

Of complex $\mu_2Cl_2[Cu_2(mbtt)_4]$

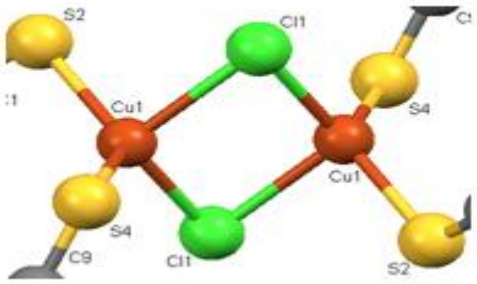

Fig. 2.4b Central unit 4-member ring

Of complex $\mu_2Cl_2[Cu_2(mbtt)_4]$

This 4 membered ring provide a basis for the complex to form a tetramer product. Both the Cu1 atoms of one half are bonded to one S atom of each ligand in the ring. The close microscopic study of the compound shows that the structure seems like a joint of two halves. There is no direct linking between two Cu atoms. The Cu-Cu bridge takes place through Cl atoms on each side. In the 4-membered ring the bond length of opposite sides Cu1—Cl1 are same as shown in table 2.2. Similarly the bond length of diagonals between Cu1—Cu1 is 3.037Å and Cl—Cl is 3.805Å. This shows that the ring is shaped as a parallelogram as shown in the Fig. 2.4c.

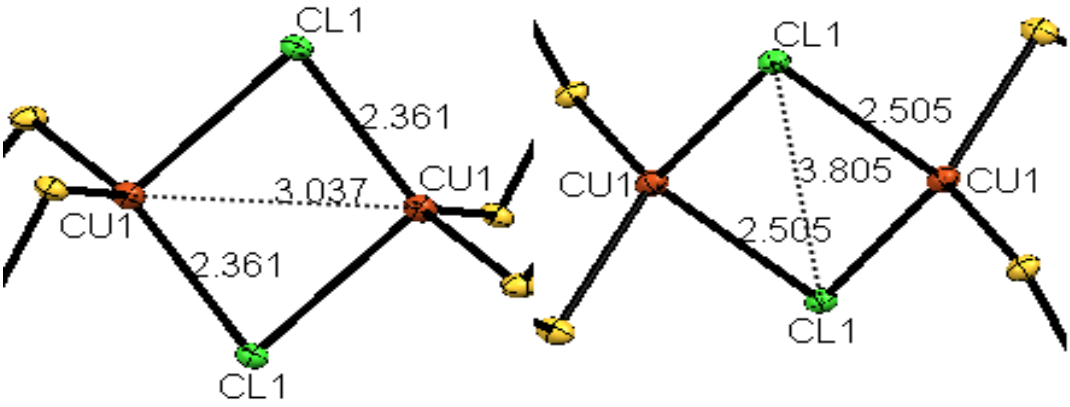

Fig. 2.4c Central complex of $\mu_2Cl_2[Cu_2(mbtt)_4]$

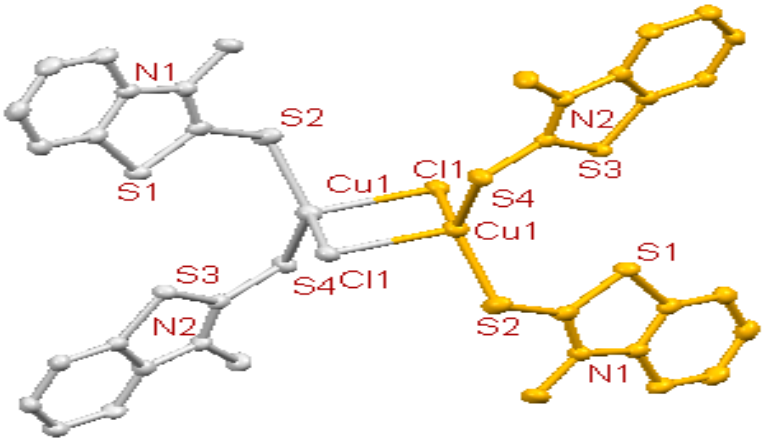

Fig. 2.5 Symmetrical structure of $\mu_2Cl_2[Cu_2(mbtt)_4]$

In the compound $\mu_2Cl_2[Cu_2(mbtt)_4]$ the two units have a symmetrical structure which are linked through Cl in central 4-membered ring. Thus the compound has its own feature in metal-heterocyclic coordination chemistry. It is observed and shown in the Fig. 2.5 that S2 and S4 are coordinated with Cu(1) from each side inversely like a mirror image. This can be seen in fig. 2.6.

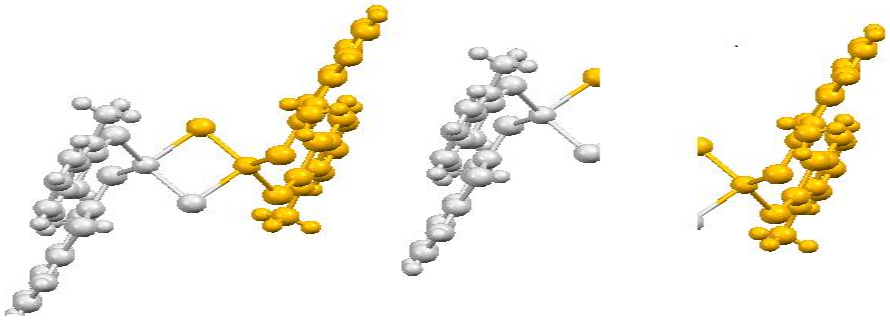

Fig. 2.6 Symmetrical inverse structure of $\mu_2Cl_2[Cu_2(mbtt)_4]$

Another aspects of the compound is that mbtt linked to Cu(I) shows a slight variation of bond length on both sides. Cu1—S2 has a bond length of 2.306 Å and Cu1—S4 has a bond length of 2.305 Å. Similarly there bond angles between Cu1—S4—C9

and Cu1—S2—C1 as shown in table 2.3 shows a slight distortion in angle which is due to the mutual repulsion between the two sulphur atoms in mbtt groups. It makes the groups slightly out of plane to attain the stability in the complex. The repulsion between S1 and S3 turns the groups out of plane and reduces the distortion between them. It is shown below in Fig. 2.7.

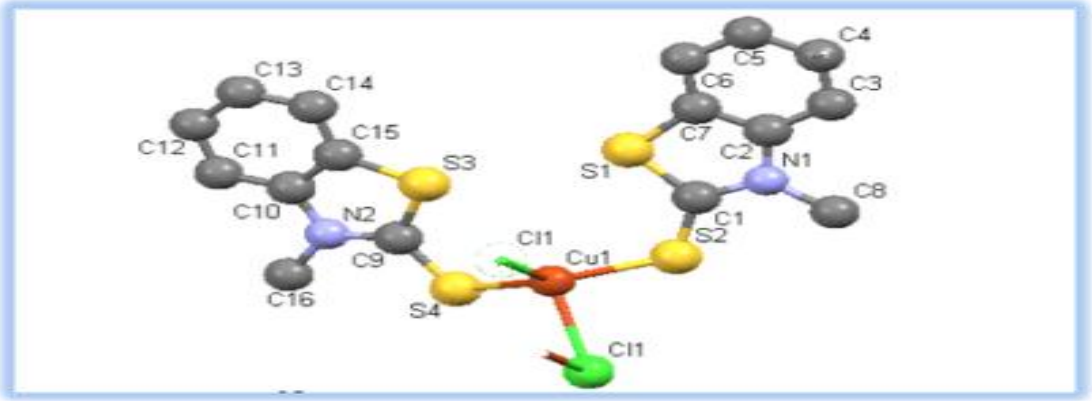

Fig. 2.7 Dimeric form of $\mu_2Cl_2[Cu_2(mbtt)_4]$

2.4.2. Intermolecular interactions in $\mu_2Cl_2[Cu_2(mbtt)_4]$

Intermolecular interaction explains the stability and properties of a compound. The compound $\mu_2Cl_2[Cu_2(mbtt)_4]$ has a strong tendency of intermolecular interactions which shows its stability behaviour. In this complex the shorter bond lengths S1—S_2 of 3.004Å, S4—N_2 of 2.707Å etc. represent its maximum stability within the compound. Hydrogen bonding is silent in the compound except an intermolecular involvement in the compound showing a bond length between H_{16a}—S_4 of 2.666Å. The other intermolecular interactions in the complex arise due to the presence of the phenyl and a 5-membered heterocyclic ring. The delocalization of charge in phenyl provides a stable structure and it is possible to have Π-Π stacking in the complex. The short contact view of the compound provides information about Π-Π stacking[9] as it is shown in Fig. 2.8 and in table. 2.4.

This strong tendency of Π-bond formation either via aromatic ring or via heterocyclic ring enhances the stability of the compound. The overall intermolecular forces are used to determine the preferred dimensions and molecular orientation of the compound.

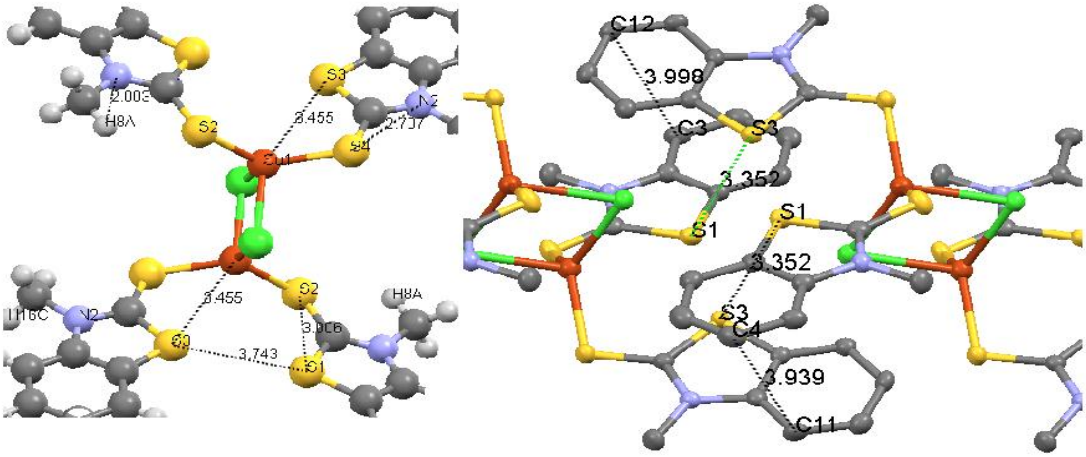

Fig. 2.8 Intermolecular interactions of $\mu_2Cl_2[Cu_2(mbtt)_4]$

Table 2.4

Intermolecular bond lengths (Å) of $\mu_2Cl_2[Cu_2(mbtt)_4]$

S1—S2	3.006 (4)	S1—S3	3.743 (5)
S3—Cu1	3.455 (4)	S4—N2	2.707 (6)
N3—H8A	2.003 (6)		
C3—C12	3.998 (6)	S1—S3	3.359 (6)
C4—C11	3.939 (6)		

2.5 Summary

The complex was synthesised under mild conditions at a very low concentrations. The use of mild conditions for reaction of copper(I) with 3 methylbenzothiazole-2-thione($C_8H_7NS_2$) in 2:1 molar ratio (M:L) in methanol yielded a dimer. The product is a colourless crystal. There is no such product is available at the Cambridge Crystallographic Data Centre (CCDC).The heterocyclic used as ligand for coinage metals especially for copper but the previous studies have dealt with Cu(II)[4] instead of Cu(I). So it can be concluded that product of Cu(I) with 3 methylbenzothiazole-2-thione (mbtt) is a novel product.

Chapter 3

X-ray Crystallographic Study of $AgNO_3$ Complex With 3-Methylbenzothiazole-2-Thione

3. Introduction

Complexes of Ag(I)NO_3 and heterocyclic compounds like 3-methylbenzothiazole-2-thione (mbtt) have not been synthesized and studied directly. Previous studies have investigated into the reactivity of 3-methylbenzothiazole-2-thione on a silver[18] surface. The research shows a surface reaction of mbtt on Ag solution to study the intermolecular rearrangement of mbtt.

The present investigation shows how $AgNO_3$ with 3-methylbenzothiazole-2-thione (mbtt) has formed a complex and a change of experimental conditions have yielded a new Ag polymer.

3.1. Experimental

3.1.1. Chemical Reagents

Pure $AgNO_3$ of analytical grade is used for the process as available in the laboratory.

Analytical grade ligand 3-methylbenzothiazole-2-thione (mbtt) has been used for the process.

Acetone and methanol (dry) are used as solvents.

3.1.2. Preparation of Reagents

A. 0.01M solution of $AgNO_3$ is prepared in Acetone.

B. 0.01M solution of 3-methylbenzothiazole-2-thione (mbtt) was prepared in methanol.

The whole procedure has been carried out under normal laboratory conditions.

3.2. Synthesis of $[Ag(mbtt)(NO_3)]_n$

The compound was prepared by direct reaction of silver nitrate (0.01M) in acetone and a solution of mbtt (0.01M) in methanol and the solution was kept unaffected for one week. The solutions are mixed in a mole ratio of 2:1. The slow evaporation of

solution at room temperature gave white colourless needle like crystals of $[Ag(mbtt)(NO_3)]_n$.

3.3. Structure Determination and Refinement

A single crystal of the compound was mounted on an X-ray Kappa APEXII diffractometer equipped with a graphite monochromator and Mo Kα radiation (λ = 0.71073 Å). The unit cell dimensions and intensity data were measured at 100K. Direct method is used to solve the structure and full-matrix least squares methods is applied to refine which is based on F^2 with anisotropic thermal parameters for the non-hydrogen atoms using CCD (data collection), SHELXS-97 (structure solution), SHELXL-97 (structure refinement) and WinGX (molecular graphics). Similarly hydrogen atoms were not refined but fixed geometrically. The chemical structure of the complex is depicted in the Fig. 3.1 and in fig. 3.1a shows its ORTEP structure.

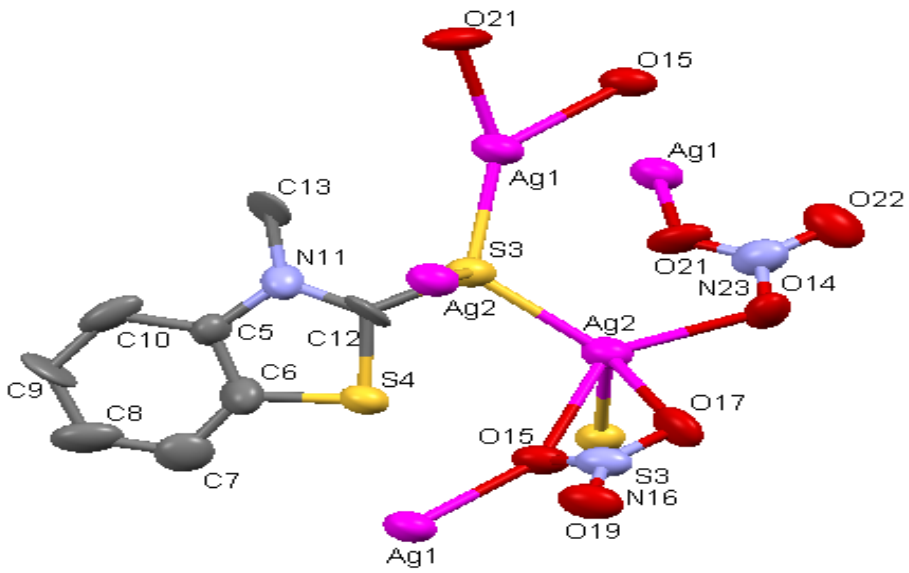

Fig. 3.1. Crystal structure of $[Ag(mbtt)(NO_3)]_n$ complex

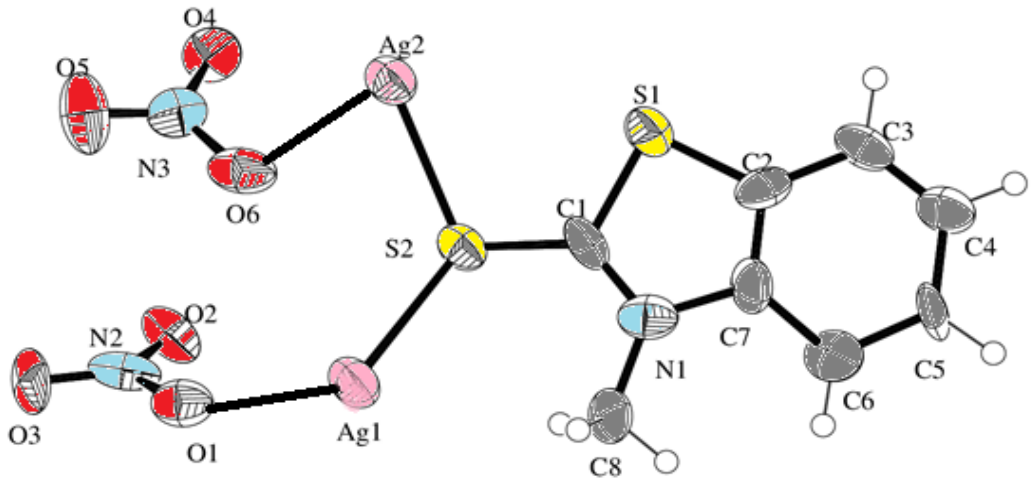

Fig. 3.1a ORTEP structure of $[Ag(mbtt)(NO_3)]_n$ complex

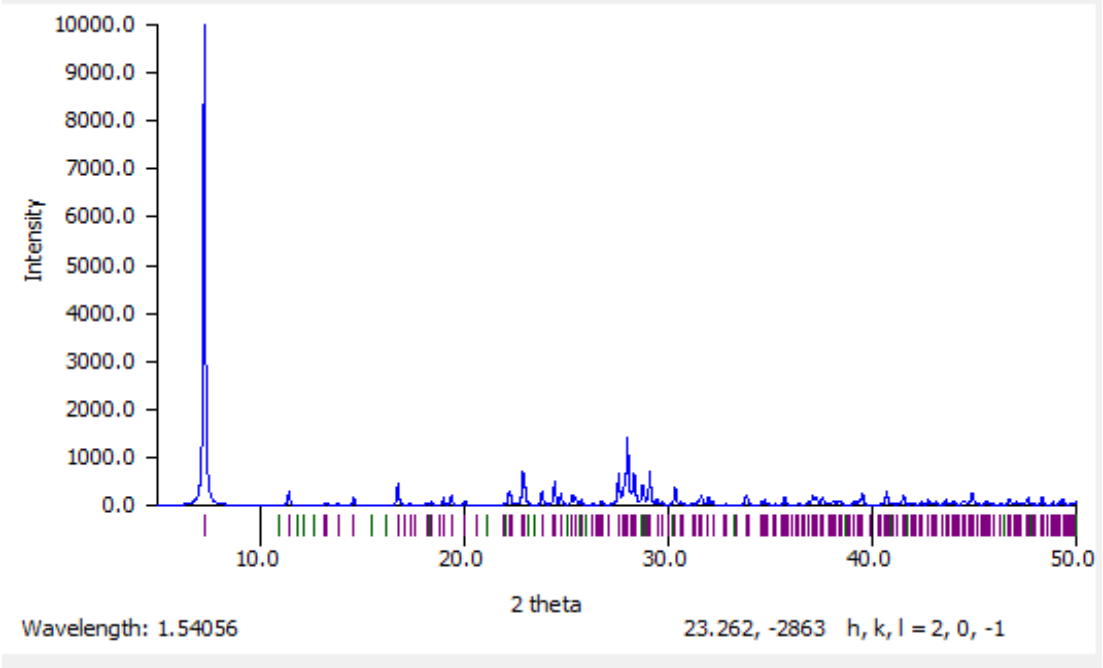

Fig. 3.1b Powder diffraction pattern of $[Ag(mbtt)(NO_3)]_n$ complex

The powder diffraction pattern of the polymeric complex were in the form of XY plot which covers '2θ' range on x-axis and Intensity were along y-axis as shown in fig. 3.1b which shows peak intensity range in between 1^{o}-50^{o}.

Similarly positional and anisotropic atomic displacement parameters were refined for all atoms except hydrogen. Hydrogen atoms were placed in different maps and included in fixed positions mounting on attached atoms with isotropic thermal parameters 1.2 times those of their transporter atoms. Criteria of a suitable complete analysis were the ratios of ''rms" change to standard deviation less than 0.001 and no significant features in final difference maps. The CIF file has been validated with Platon program. A summary of the crystal data along with further details of the structure for complex and the atomic coordinates along with their equivalent isotropic displacement parameters are presented in table 3.1.

Table 3.1

Crystal data of $AgNO_3$ with 3-methylbenzothiazole-2-thione complex

Parameters	Description	Parameters	Description
Empirical formula	$C_8H_7Ag_2N_3O_6S_2$	Density D_x	2.645 Mg m^{-3}
Molecular mass M_r	521.03	Cell parameters	2338 reflections
Crystal system	Monoclinic	Mo $K\alpha$ radiation, λ	0.71073 Å
Space group	$P2_1/c$	Cell reflections I	1299
Nature of crystals	Colourless, needle	Z	4
a	7.7373 (6) Å	μ	3.34 mm^{-1}
b	6.9824 (6) Å	T	100 K
c	24.246 (2) Å	wR	0.238
β	92.534 (4)°	R	0.093
Cell volume V	1308.60 (19) $Å^3$	R_{int}	0.093

.

The structure of $[Ag(mbtt)(NO_3)]_n$ is in a monoclinic crystal system space group $P2_1/c$ with the cell parameters as given in table 2.1. The structure was refined to the final R1 = 0.093 using all 2338 observed reflections. The complex shows covalent bonding with Ag atom bonded to mbtt molecule. A summary of selected bond length and bond angles of the structure along with symmetry codes is given in table 3.2 and table 3.3 respectively.

Table 3.2.

Bond lengths of $[Ag(mbtt)(NO_3)]_n$ complex

Parmeter	Bond Length(Å)	Parmeter	Bond Length(Å)
C1—N1	1.32 (3)	Ag1—O6^{i}	2.311 (14)
C1—S2	1.72 (2)	Ag1—S2	2.446 (5)
C1—S1	1.746 (19)	Ag2—O4	2.405 (15)
C2—C7	1.35 (3)	Ag2—S2	2.511 (5)
C2—S1	1.71 (2)	Ag2—S2^{ii}	2.586 (6)
C7—N1	1.43 (3)	N2—O3	1.22 (2)
N2—O2	1.29 (2)	N2—O1	1.28 (2)
C8—N1	1.44 (2)		
Symmetry codes: (i) $-x+2, y+1/2, -z+1/2$; (ii) $-x+1, y-1/2, -z+1/2$			

Table 3.3

Bond angles of $[Ag(mbtt)(NO_3)]_n$ complex

Parameter	Bond Angle (Å)	Parameter	Bond Angle (Å)
N1—C1—S2	128.1 (16)	O1—Ag1—S2	136.1 (3)
N1—C1—S1	112.4 (15)	O4—Ag2—S2	120.8 (4)
S2—C1—S1	119.4 (13)	O3—N2—O1	119.5 (17)
C7—C2—C3	119.0 (18)	O5—N3—O4	120.7 (19)
C7—C2—S1	110.8 (16)	C1—S2—Ag1	119.8 (7)
C3—C2—S1	130.0 (16)	C1—S2—Ag2	108.0 (8)
C2—C7—N1	114.1 (18)	Ag1—S2—Ag2	116.8 (2)
N1—C7—C6	121.0 (19)	N2—O1—Ag1	106.2 (12)
N3—O6—Ag1^{iv}	121.9 (13)	N3—O4—Ag2	106.1 (12)

Symmetry codes: (i) $-x+2, y+1/2, -z+1/2$; (ii) $-x+1, y-1/2, -z+1/2$; (iii) $-x+1, y+1/2, -z+1/2$; (iv) $-x+2, y-1/2, -z+1/2$.

The compound $[Ag(mbtt)(NO_3)]_n$ has needle like crystals having monoclinic crystal system. The Ag atom in the group may show variance in coordination as Ag belongs to $3d^{10}$ systems in transition metals. The complex is found to be monomeric and asymmetric. The silver atoms present in the compound as Ag1 and Ag2 are joined together through S2 of 3-methylbenzothiazole-2-thione. Ag acts as a bridge between nitrate and ligand mbtt as shown in Fig. 3.1. The silver atoms show a variation of bond angles as depicted in Table 3.3.

The unit cell contains 3 units, which stack in a highly ordered packing along the 001 axis throughout the crystal system. The short contact view of the compound provides information about its preferred dimensions, molecular orientation, and approximate linearity as shown in Fig. 3.2.

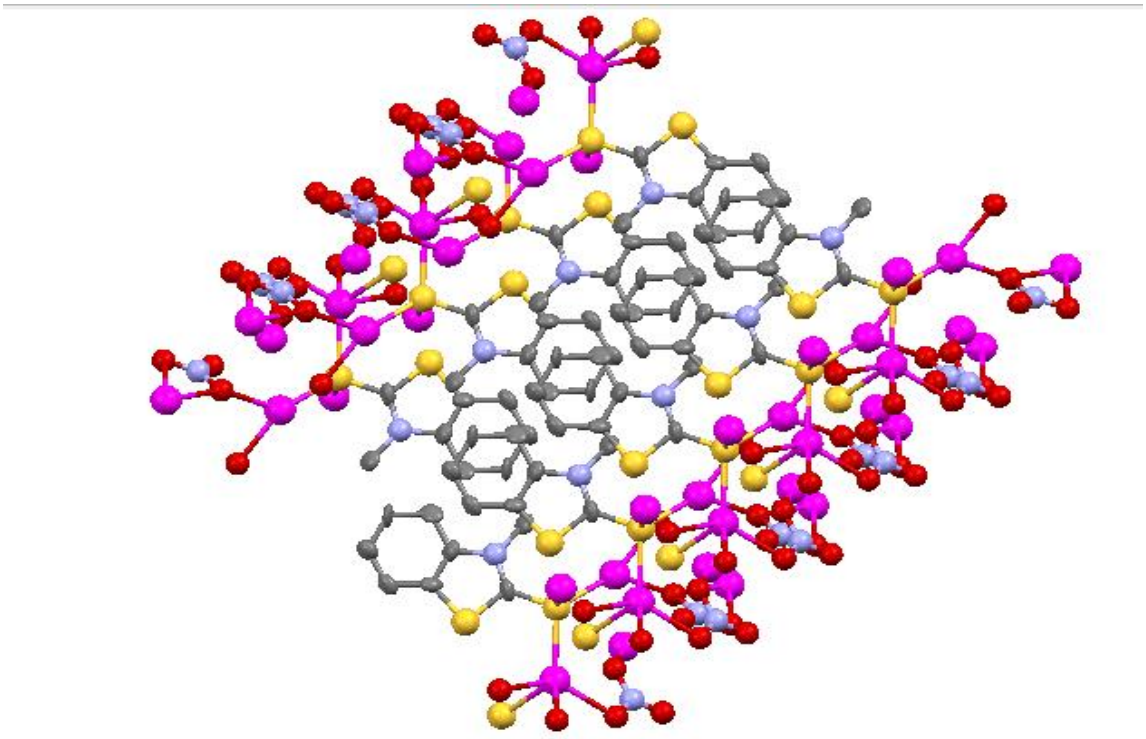

Fig. 3.2 Crystal structure of $[Ag(mbtt)(NO_3)]_n$ complex

A space filling model of this structure reveals how very sterically hindered the Ag atoms are, as shown in fig.3.3. This reinforces the idea of the Ag atom playing only a structural role in the complex.

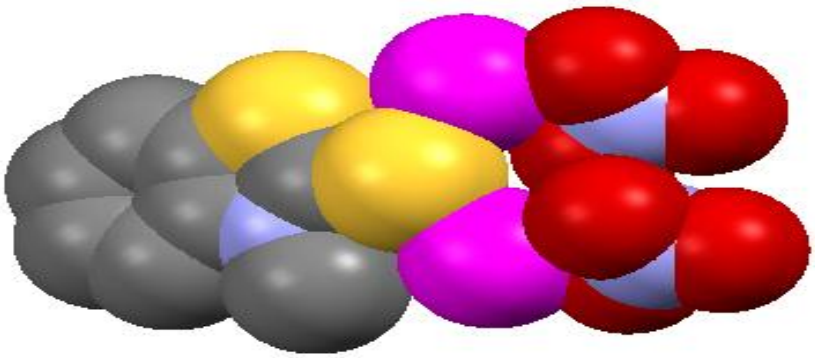

Fig. 3.3 Space filling model of $[Ag(mbtt)(NO_3)]_n$ complex

3.4. Results and Discussion

3.4.1. General view about $[Ag(mbtt)(NO_3)]_n$ complex structure

The compound $[Ag(mbtt)(NO_3)]_n$ has a monoclinic crystal system. The silver atoms linked to the ligand though sulphur atoms from different sides shows some variation in bond length as well bond angle as given in Table 3.3 and in fig. 3.4.

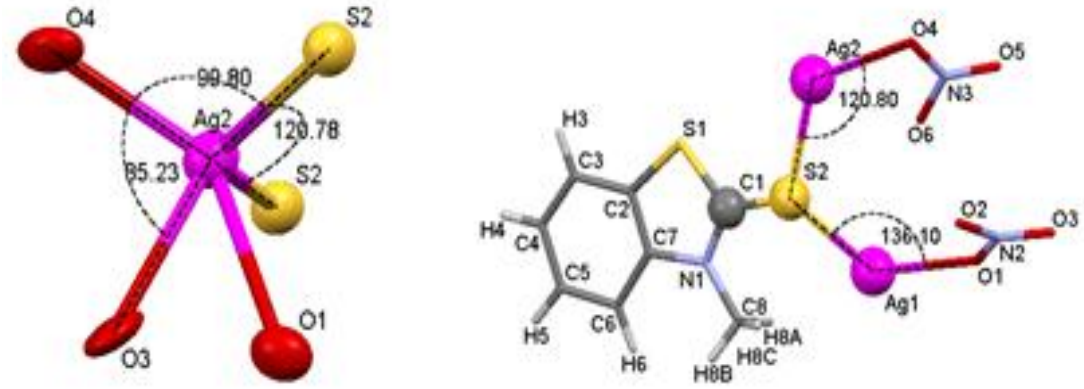

Fig. 3.4 Bond angles of $[Ag(mbtt)(NO_3)]_n$ complex

3.4.2. Single crystal structures of complex

The complex $[Ag(mbtt)(NO_3)]_n$ has a polymer structure as shown in fig.3.5. Crystallographically silver atoms are involved to develop a link between the ligand and nitrate groups and bond length between them shows this aspect Ag2—O4 of 2.405Å, Ag2---S2 of 2.511Å. Sulphur atom act as a centre between ligand and the silver group and shows tetrahedral bonding. In the same way silver shows its variable bonding in the complex to develop a polymer linking to from a polymer complex as shown in fig. 3.5 and fig. 3.1

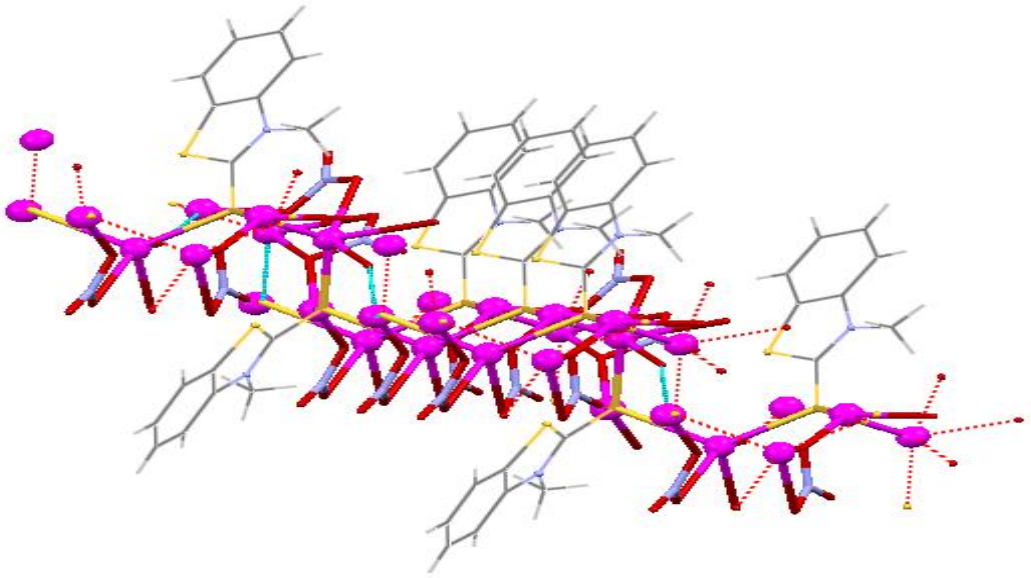

Fig. 3.5 A polymer of $[Ag(mbtt)(NO_3)]_n$

3.4.3. Intermolecular interactions in $[Ag(mbtt)(NO_3)]_n$

Intermolecular interaction explains the stability and properties of a compound. These forces can affect physical and chemical properties of the compound. Hydrogen bonding is quite effective in $[Ag(mbtt)(NO_3)]_n$. It is due to the presence of oxygen on nitro group and sulphur atoms in the ligand. Both oxygen and sulphur have key roles in developing hydrogen bonding. The bond length between H3—O2 is 2.704Å and that of H8A—O5 is 2.988Å as shown in Fig. 3.6. The shorter the bond length the more effective is the intermolecular force. Thus the presence of shorter bond length between hydrogen and the highly electronegative elements i.e. oxygen and sulphur shows the high stability of $[Ag(mbtt)(NO_3)]_n$. The compound $[Ag(mbtt)(NO_3)]_n$ has a strong tendency of intermolecular interactions which shows its stability behaviour. In this complex the shorter bond lengths represent its maximum stability within the compound as given in table 3.2.

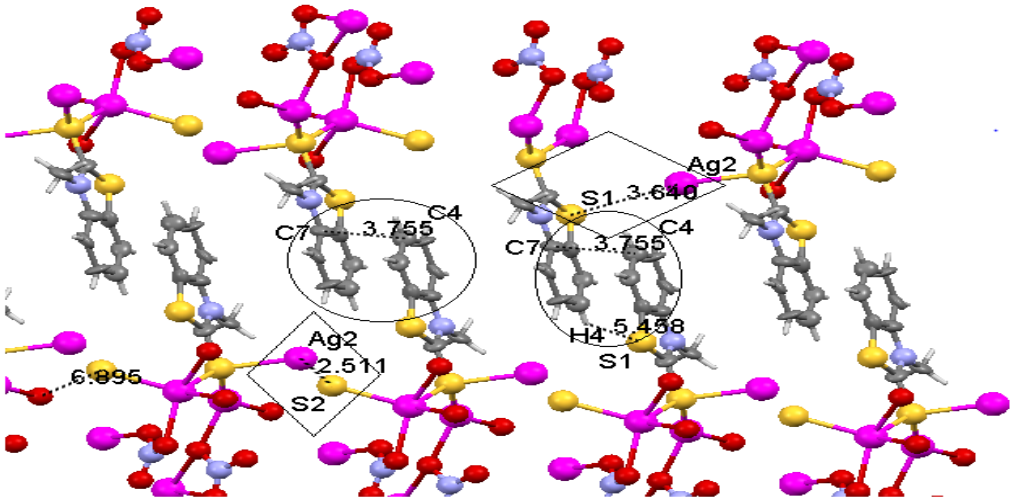

Fig. 3.6 Intermolecular bond length of $[Ag(mbtt)(NO_3)]_n$ complex

The other intermolecular interactions in $[Ag(mbtt)(NO_3)]_n$ arise due to the presence of Π bonds available in the benzene ring. There is a delocalization of the charge due to this Π-bond in adjacent groups as shown by circles in fig. 3.6. This explains the stable behaviour of the structure and it is possible to have Π-Π stacking in the adjacent groups as in C7—C4 it is 3.755 Å which is less than the Van der Waals distance range i.e. 4.0Å for pi-pi interactions. Similarly the short contact view of

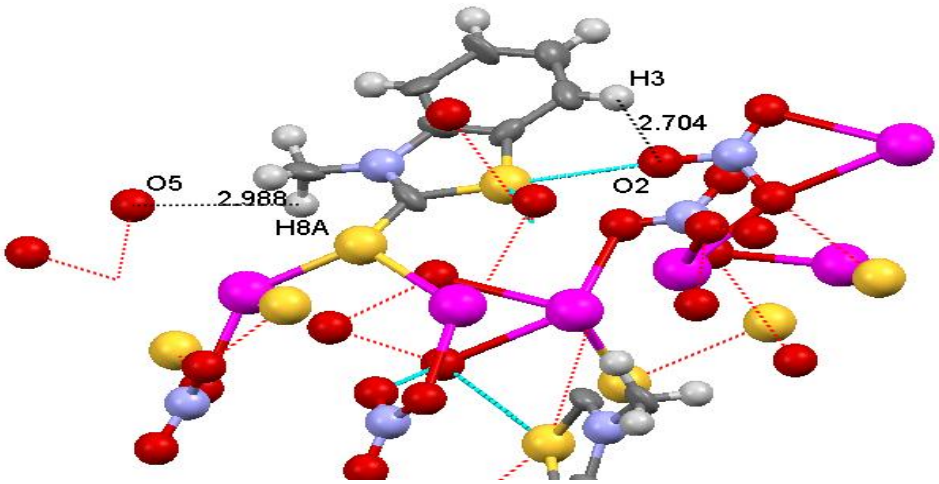

Fig. 3.7 Intermolecular bond length of $[Ag(mbtt)(NO_3)]_n$ complex

$[Ag(mbtt)(NO_3)]_n$ also provides information about Π-Π stacking[9] as it is shown in Fig. 3.7. This tendency of Π-bond formation in benzene and the interactions of hydrogen bonding also explain the stability of the compound. The overall intermolecular forces are used to determine the preferred dimensions and molecular orientation of the compound.

3.5. Summary

The complex was synthesised under mild conditions at a very low concentrations.
The use of mild conditions for reaction of $AgNO_3$ with 3-methylbenzothiazole-2-thione ($C_8H_7NS_2$) in 2:1 molar ratio (M:L) in acetone/methanol yielded a polymer. The product is a colourless crystal. There is no such product is available at the Cambridge Crystallographic Data Centre (CCDC).Formerly the silver solution has been used to study the intermolecular rearrangement of 3- methylbenzothiazole-2-thione[19]. So it can be concluded that product of $AgNO_3$ with 3 methylbenzothiazole-2-thione is a new product.

Chapter 4

X-ray crystallographic study of

Di-2-Thienylmethanone

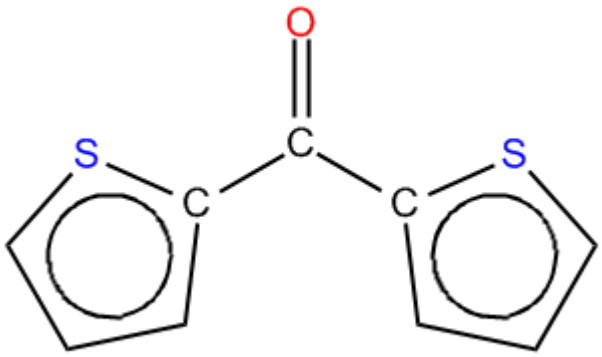

4.1. Introduction

This compound was obtained randomly while working on Coinage metal and substituted thiourea complexes. Thus the synthesis and crystallographic data of these needles like crystals were also studied. This was produced by adding Bi-pyridole (ketone) to a solution of the reagents of copper(I)chloride and substituted thiourea. Single crystal X-ray diffraction has been used to study the crystallographic properties of the product obtained.

4.2. Experimental

4.2.1. Preparation of reagents

Following solutions were prepared in Methanol:
A. 0.01M solution of Cu(I)Cl.
B. 0.01M solution of substituted thiourea.
C. 0.01M solution of Bi-pyridole(a ketone)
The whole procedure was carried out under normal laboratory conditions.

4.3. Synthesis of Di-2-thienylmethanone

All the reagents were mixed together in non-stoichiometric ratio and left to react uninterrupted for one week. On mixing, the solution turned to dark blue. The slow evaporation of the solution at room temperature gave colourless prismatic needle like crystals of the product.
The study focuses on the intriguing behaviour of side products of copper(I)chloride with substituted thiourea in the presence of Bi-pyridole (a ketone).

4.4. Structure Determination and Refinement

A single crystal of compound was mounted on an X-ray Kappa diffractometer equipped with a graphite monochromator and Mo Kα radiation (λ = 0.71073 Å). The unit cell dimensions and intensity data were measured at 100K. The structure was solved by the direct methods, and refined by the full matrix least squares based on F^2 with anisotropic thermal parameters for the atoms except non-hydrogen using CCD (data collection), SHELXS-97 (structure solution), SHELXL-97 (structure refinement) and WinGX (molecular graphics). A crystal structure is obtained from the data as displayed below in fig. 4.1 and fig. 4.1a represents its ORTEP structure.

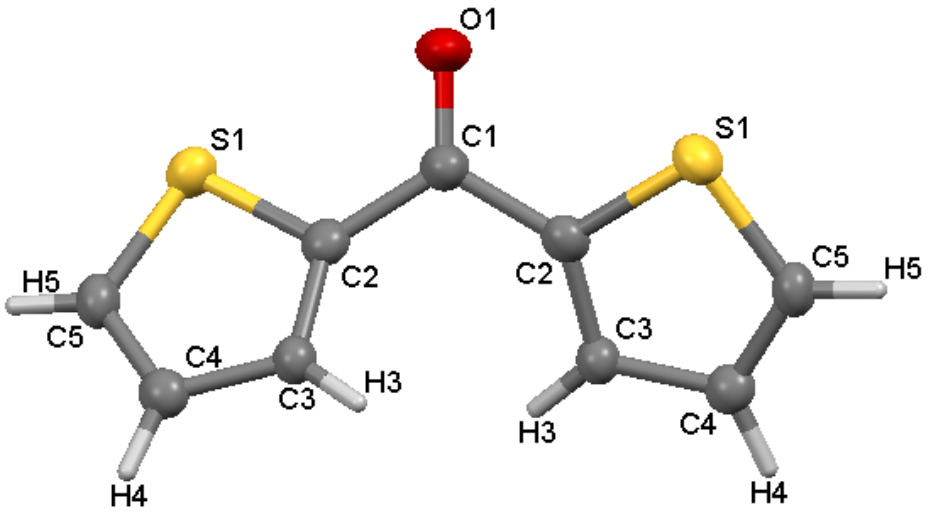

Fig. 4.1 Crystallographic structure of Di-2-thienylmethanone

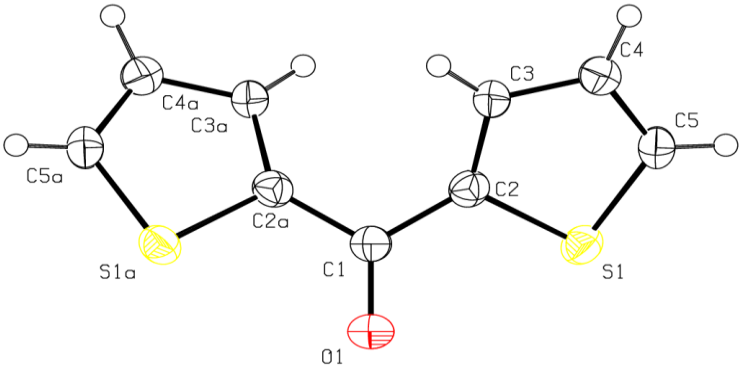

Fig. 4.1a ORTAP structure of Di-2-thienylmethanone

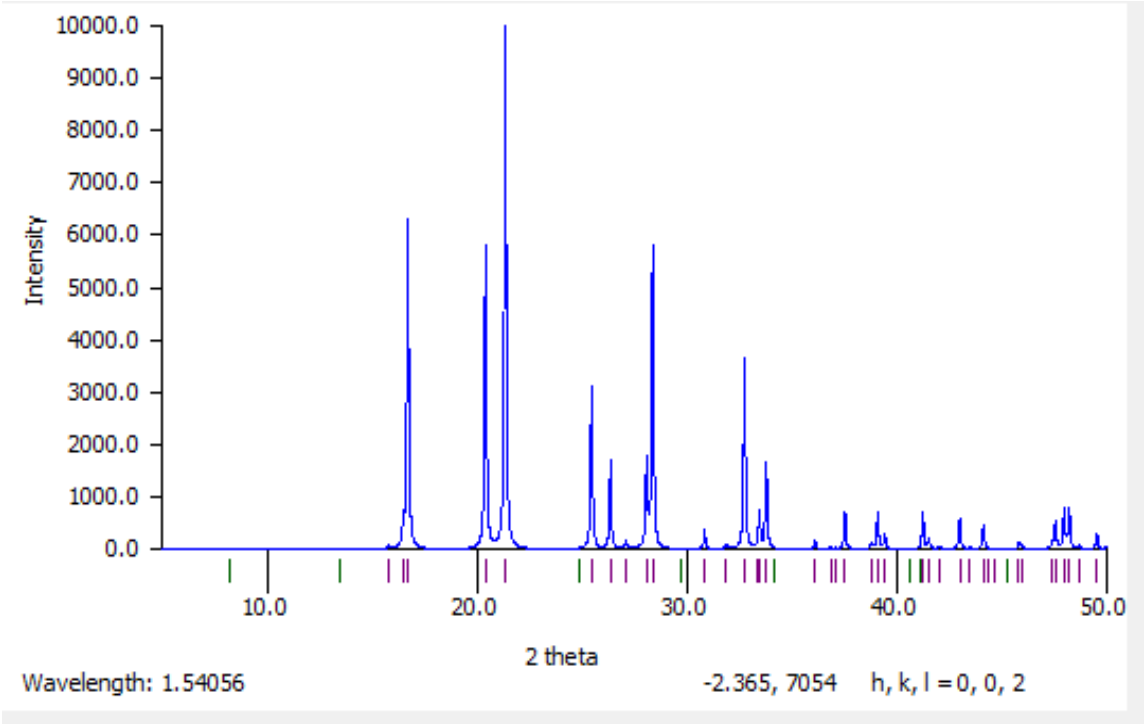

Graph 4.1 Powder diffraction graph of di-2-thienylmethanone

Similarly the powder diffraction pattern of the compound in the form of XY plot which covers '2θ' range on x-axis and Intensity along y-axis as shown in graph 4.1 which shows peak intensity range in between 15^{o}-50^{o}.

All positional and anisotropic atomic displacement parameters were refined for atoms except hydrogen atoms. Hydrogen atoms were located in different maps and included in fixed places riding on attached atoms with isotropic thermal parameters 1.2 times those of their carrier atoms. Criteria of a suitable complete analysis were the ratios of ''rms" shift to standard deviation less than 0.001 and no significant features in final difference maps. The general crystallographic data for complex is given in table 4.1.

Table. 4.1

Crystallographic data of Di-2-thienylmethanone

Parameter	Description	Parameter	Description
Empirical Formula	$C_9H_6OS_2$		
M_r	194.26	D_x	1.519 Mg m^{-3}
Crystal system	Orthorhombic		
Space group	*F2dd*	Mo *Kα* radiation, λ	0.71073 Å
Nature of Crystal	Prism, colourless	Cell parameters from	810 reflections
a	6.0162 (4) Å	Cell Reflection *I*	879
b	13.1522 (10) Å	μ	0.57 mm^{-1}
c	21.4772 (19) Å	*T*	100 K
B	90°	*Z*	8
V	1699.4 (2) $Å^3$	*R*	0.041
R	0	*wR*	= 0.110

Similarly crystallographic data for complex regarding bond length and bond angle with symmetry codes is given in table 4.2 and table 4.3 respectively.

Table. 4.2

Bond lengths of Di-2-thienylmethanone

Parameter	Bond Length(Å)	Parameter	Bond Length(Å)
C1—O1	1.229 (7)	C3—H3	0.91 (4)
C1—C2^{i}	1.467 (4)	C4—C5	1.366 (5)
C1—C2	1.467 (4)	C4—H4	0.94 (4)
C2—C3	1.380 (4)	C5—S1	1.706 (4)
C2—S1	1.741 (3)	C5—H5	0.90 (3)
C3—C4	1.418 (4)		
Symmetry code: (i) x, $-y+1/2$, $-z+1/2$.			

Table. 4.3

Bond angles of Di-2-thienylmethanone

Parameter	Bond Angle (Å)	Parameter	Bond Angle (Å)
O1—C1—C2^{i}	121.6 (2)	C4—C3—H3	130 (3)
O1—C1—C2	121.6 (2)	C5—C4—C3	112.3 (3)
C2^{i}—C1—C2	116.9 (5)	C5—C4—H4	123 (2)
C3—C2—C1	130.3 (3)	C3—C4—H4	125 (2)
C3—C2—S1	111.1 (2)	C4—C5—S1	112.9 (2)
C1—C2—S1	118.3 (3)	C4—C5—H5	126 (3)
C2—C3—C4	112.5 (3)	S1—C5—H5	121 (3)
C2—C3—H3	118 (3)	C5—S1—C2	91.22 (16)
Symmetry code: (i) x, $-y+1/2$, $-z+1/2$.			

The compound has orthorhombic crystal system with space group F2dd. It is separated in the dark blue solution as fine needle like crystals. The unit cell stacks in a highly ordered packing along the 001 axis throughout the crystal system. The short contact views of the compound provide information about its preferred dimensions, molecular orientation and approximate linearity as shown in fig. 4.3.

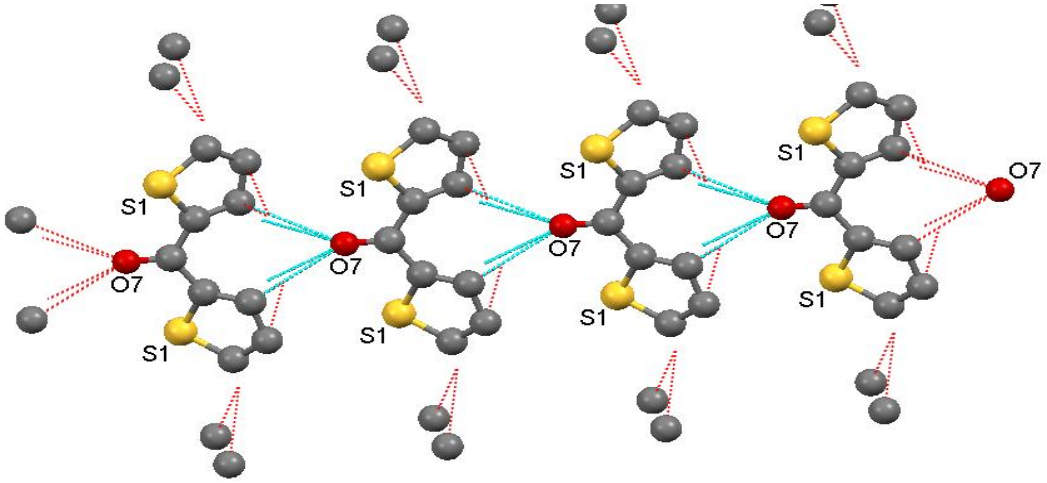

Fig. 4.3 Unit Cell structure of Di-2-Thienylmethanone

A space filling model of this structure reveals how very sterically hindered the compound is, as shown in fig. 4.4. This reinforces the idea of the carbonyl group playing only a structural role in the complex.

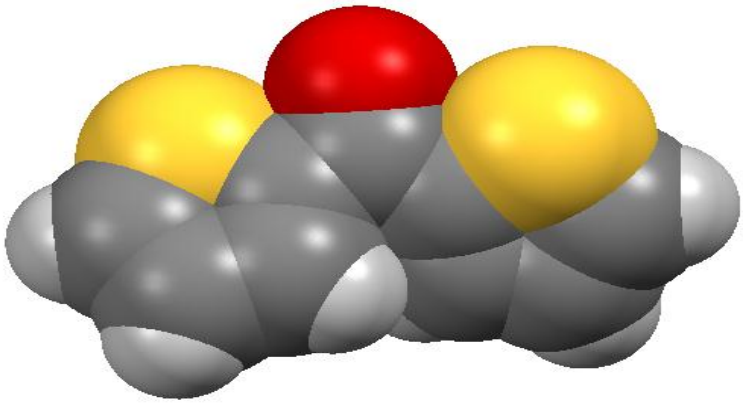

Fig. 4.4 Space filling model of complex of Di-2-Thienylmethanone

4.5. Results and discussion

4.5.1. Crystallographic study of Di-2-Thienylmethanone

The observation of unit cell structure as in fig. 4.3 shows the polymeric nature of the compound Di-2-thienylmethanone. The thiophenyl group links to the carbonyl group via carbon to form a ketone. The close microscopic study of the compound shows that the structure seems like a joint of two halves with a slight variation of angle. The bond angles are:

S1—C5—C6	117.75^{o}
C5—C6—O7	121.79^{o}
C5—C6—C5	116.42^{o}

Sulphur does not take part in any direct linking to the carbonyl group (Fig. 4.5).

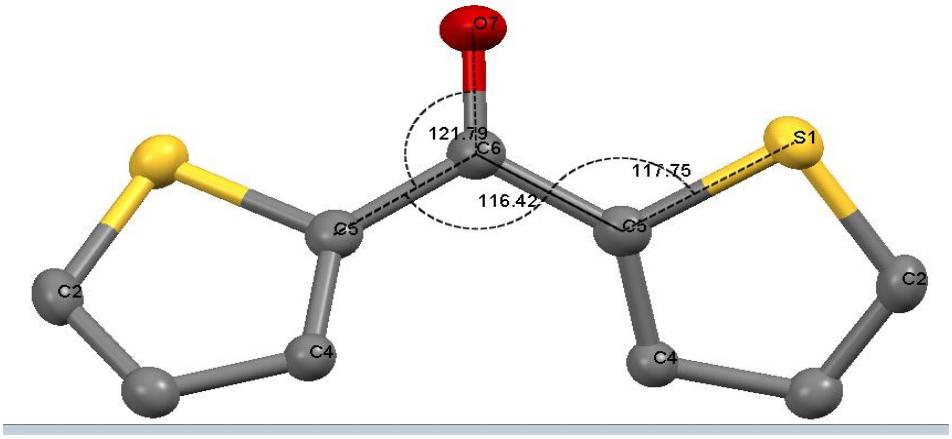

Fig. 4.5 Bond angle of Di-2-thienylmethanone

This is a symmetrical product having a twist in the bond which is due to the presence of two thiophenyl groups attached to carbonyl group. These groups are bonded with the carbonyl group in such a way that the sulphur atom, in both rings, is placed next to the bonded carbon atom. Thus the compound has its own feature in carbonyl group synthesis as shown in fig. 4.6.

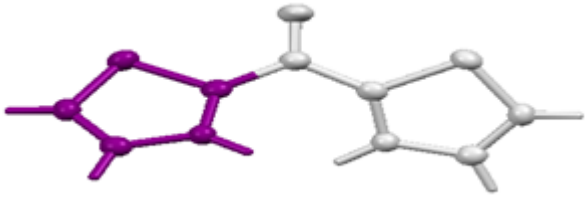

Fig. 4.6 Symmetrical structure of Di-2-thienylmethanone

4.5.2. Intermolecular interactions in Di-2-Thienylmethanone

Intermolecular interaction explains the stability and properties of a compound. These forces can affect physical and chemical properties of the compound. Hydrogen bonding is quite effective in Di-2-thienylmethanone. It is due to the presence of oxygen on the carbonyl group and sulphur in both thiophenyl rings. Both oxygen and sulphur have key roles in developing hydrogen bonding which is normally 4.0 Å. The bond length between H3—S1 is 3.126Å and that of H4 — O7 is 2.515Å which is shorter than the standard value as shown in fig. 4.7. The shorter the bond length the more effective is the intermolecular forces. Thus the presence of shorter bond length between hydrogen and the highly electronegative elements i.e. oxygen and sulphur shows the high stability of Di-2-thienylmethanone.

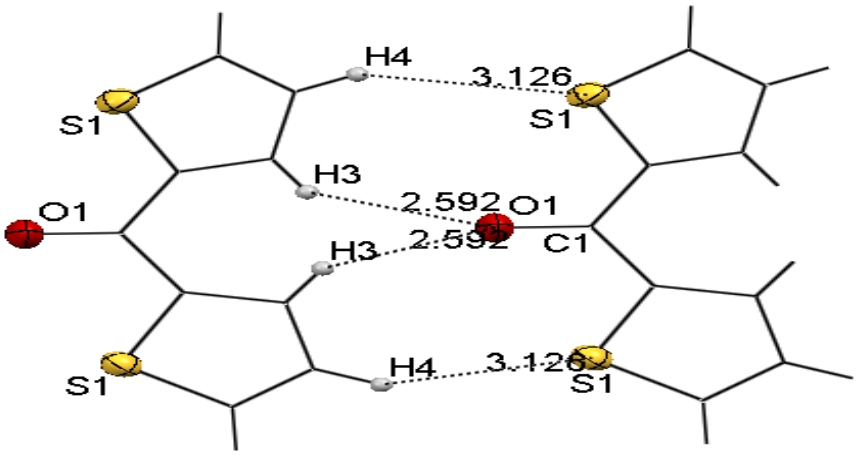

Fig. 4.7 Intermolecular Bond Length of Di-2-thienylmethanone

Similarly the intermolecular interactions in Di-2-thienylmethanone arise due to the presence of Π electronic cloud available in the thiophenyl ring which behaves as aromatic system. Side wise interactions arise due to the Π-electron system of the aromatic group and the hydrogen atom. The bond length in the complex as in C3—H5 is 2.799 Å, C4—H5 is 2.846 Å which is shorter than the standard value .i.e. 4.00Å. This shorter bond length shows maximum stability of Di-2-thienylmethanone and provides information about side wise pi-H[9] interaction in the complex as it is shown in fig. 4.8. The tendency of Π-H bond formation in thiophenyl group as an aromatic system and the interactions of hydrogen bonding explain the stability of the compound. The overall intermolecular forces are used to determine the preferred dimensions and molecular orientation of the compound.

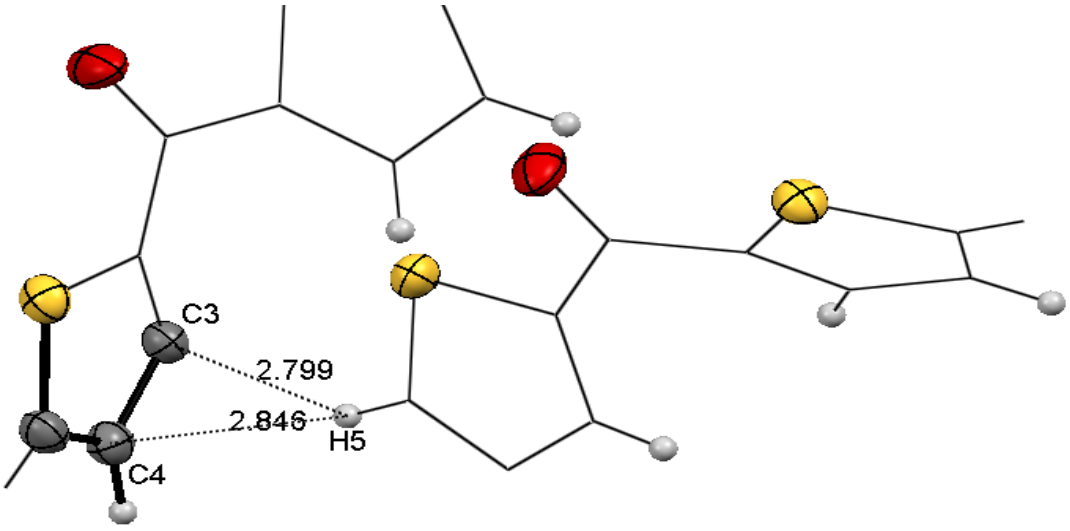

Fig. 4.8 Intermolecular Bond Length of Di-2-thienylmethanone

4.6. Summary

The compound Di-2-thienylmethanone ($C_9H_6S_2O$) was synthesised under mild conditions at very low concentrations. Although there are three different compounds on the data base having the same molecular formula i.e. $C_9H_6S_2O$ but Di-2-Thienylmethanone has a different structure arrangement. Thus it can be said that the compound Di-2-Thienylmethanone is the isomeric[20] form of the existing compounds as given in fig. 4.9

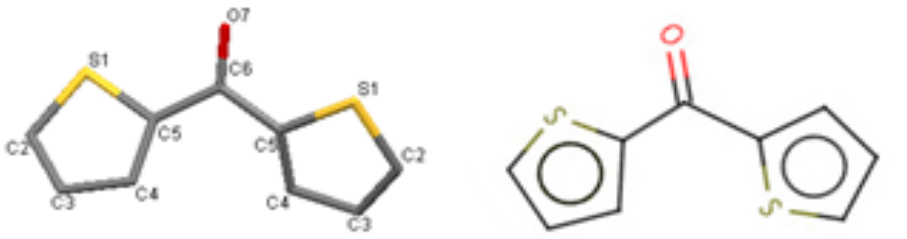

bis(thiophen-2-yl)methanone; Di-2-thienylmethanone

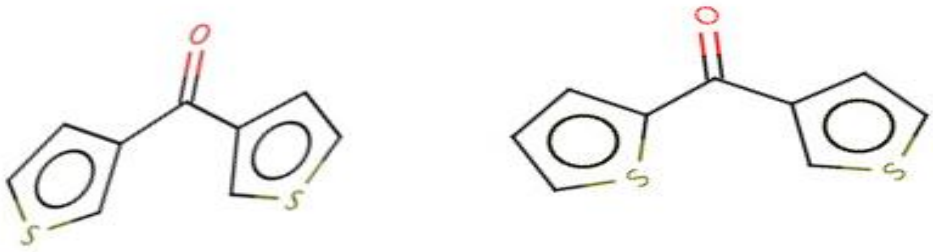

di(3-thienyl)methanone **2-thienyl(3-thienyl)methanone**

Fig. 4.9 existing isomers[21] of

Di-2-thienylmethanone on the database

Chapter 5

X-ray Powder diffraction study of copper(I) Thiourea complex

5.1. Introduction

The Cu(I)-thiourea complex precipitated with different stoichiometric compositions as anhydrous or hydrated forms has already been synthesized previously[1]. In this report the structures of 1:1 complex of Cu(I) with thiourea described. The 1:1 complex of Cu(1)Cl and thiourea in methanol is made by using a new and different procedure. This whole attempt is made in a solution of very low concentration of 0.01M to study the formation and behaviour of the compound. It is interesting that the product is in powder form and is completely different in appearance and behaviour from the existing compounds and is not available in CCD.

5.2. Experimental

5.2.1. Preparation of chemical reagents

Solid Cu(1)Cl was dissolved in dry methanol to prepare solution of 0.01M which is a very low concentration solution. The Cu(1)Cl solution is partially soluble, so for the process it should be well shaked and proper filtration to get a pure solution.
On the other hand prepare 0.01M solution of thiourea in dry methanol.

5.3. Synthesis of Cu-Thiourea complex

The solutions were mixed at a stoichiometric ratio of 1:1 to carry out the reaction. It precipitated readily on mixing. The precipitate was allowed to dry for some time and then filtered off. The whole procedure was carried out at room temperature.

5.4. Structure determination and refinement

This 2D powder pattern (graph 5.1) which is also called fingerprint pattern of compound is obtained from D8 Bruker powder diffractometer with specific wavelength of Cu Kα, λ = 1.5418Å. A '2θ' scale for these scans were observed between 5-40° with 0.6° diversion and anti-diversion slits, increment was 0.06° and scan speed was 18°/min. Sample in white powder form was placed on silicon plate which provides a clear background without any additional and extra peaks. A microscope slide was used to make sample surface flat on silicon plate because wavelength of Cu Kα, λ = 1.5418Å needs smooth surface to interact directly with sample. The powder sample of Cu(1)Cl and thiourea (tu) with molar ratios 1:1 is analysed.

The results were in the form of XY plot which covers '2θ' range on x-axis and linear count (Intensity) were along y-axis. In these graphs peak intensity over '2θ' pattern is diagnostic of the materials being studied. However all ten diffraction patterns can be plotted independently for each sample but separate interpretation and comparison of all these plots would be challenging. So new crystalline phases could be spotted more easily by making combined graph using all ten sample patterns. However, all those results were combined in 2D pattern (graph 5.1) with the help of EVA software. EVA is software in powder diffractometer which presented the results in the form of colourful pattern. Basically these colours illustrate the intensity of material. More sharp and intense colours indicated as highly intense and sharp peaks.

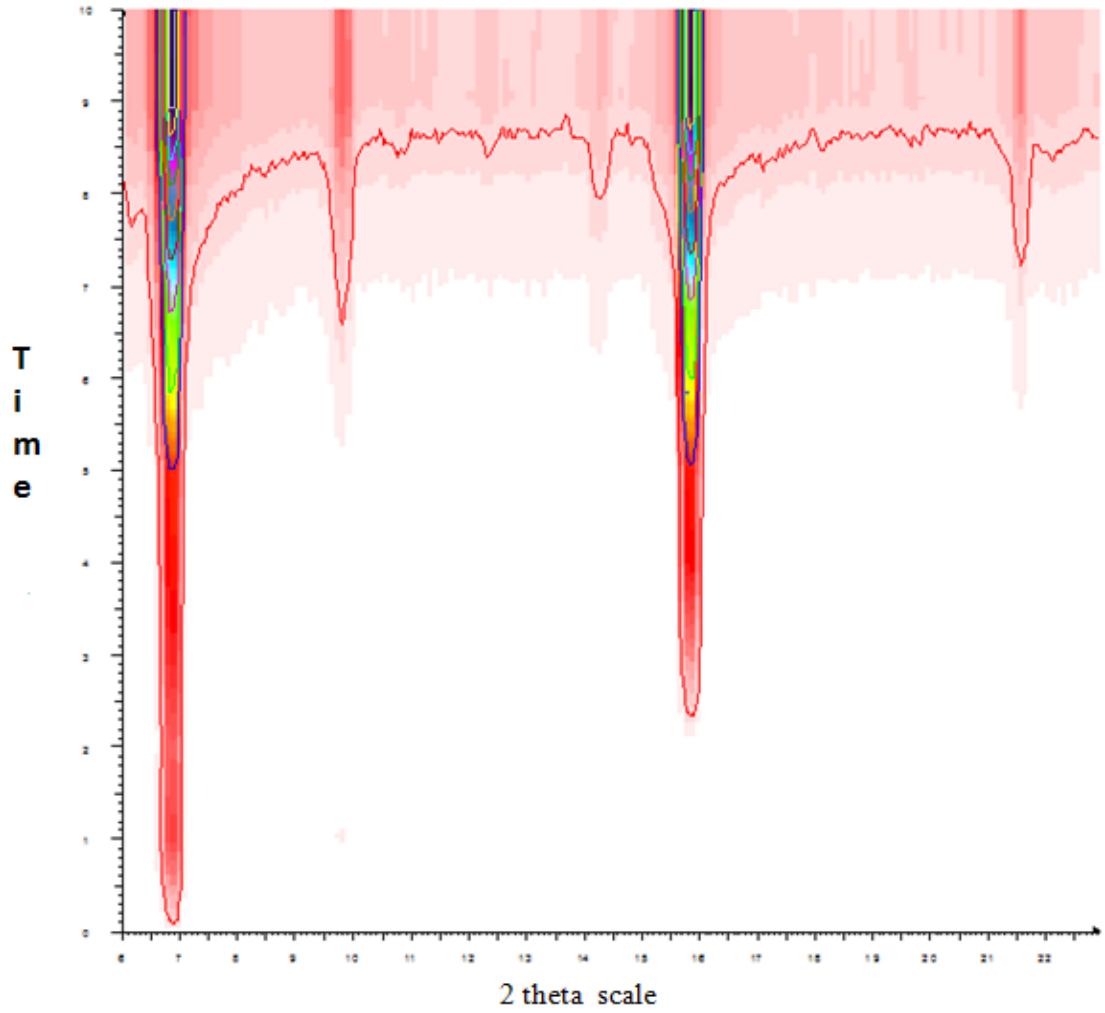

Graph 5.1 2D powder pattern of Cu(1)Cl and thiourea (tu)

This pattern in graph5.1 is identifying peaks of new compound. While colour is changing from red to black that indicates the intensity of peaks. The prediction of this pattern explains that if the sample consists of two phases, the resulting pattern would contain peaks from both materials or it may be prediction of a new compound.

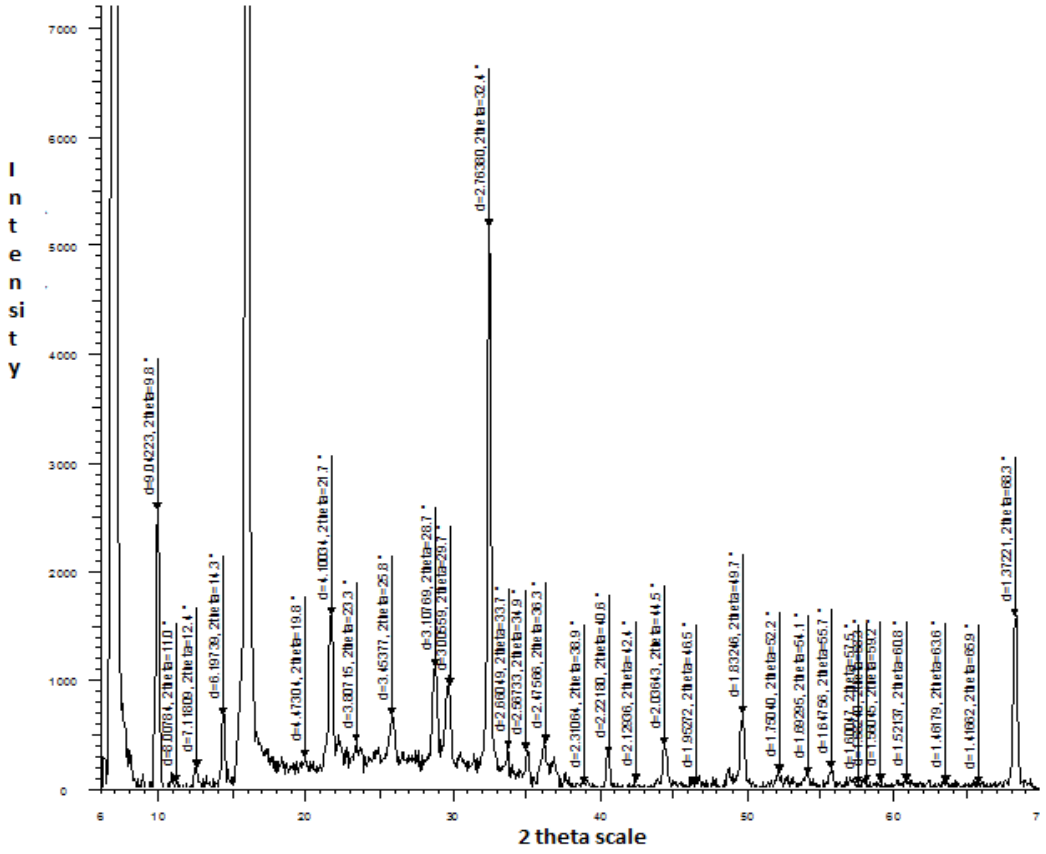

Graph 5.2 1D powder pattern of Cu- thiourea for 'd' and 'θ' value

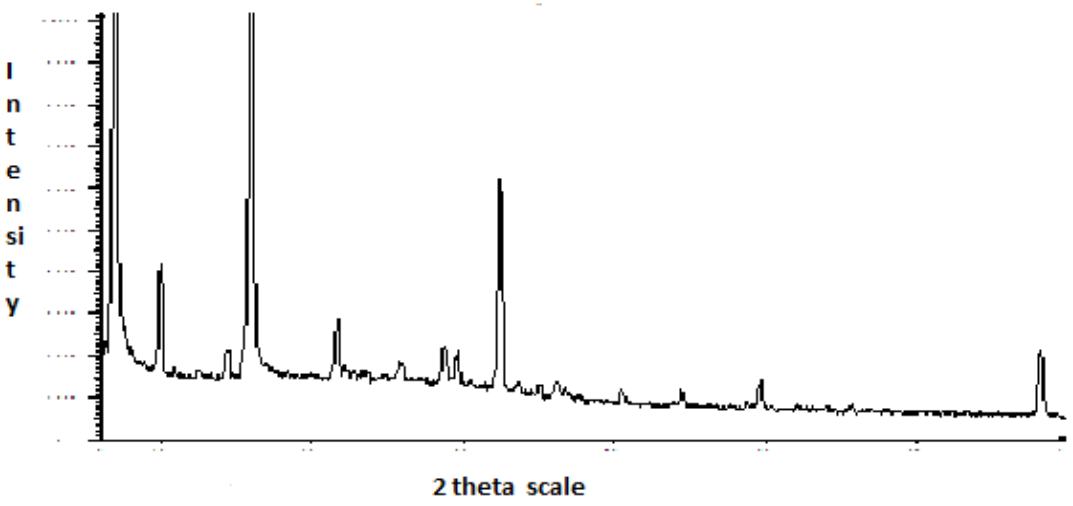

Graph 5.3 1D powder pattern for 'd' and 'θ' value

of Cu(1)Cl and thiourea (tu)

The values of ‘d’ spacing and ‘2θ’ are calculated from graph 5.2 and 5.3‘for further predictions of the complex. The powder diffractometer provides the information related to the compound to be investigated in the form of graph. This is shown in graph 5.1 which is helpful in calculating the basic values like ‘d’ spacing and ‘2θ’.

5.5. Results and discussion

All the available data is then used to calculate different parameters of unit cells, volume of the conventional cell etc. Cell refinement is done by a programme PIRUM or PURUM which is a software used to identify different parameters. This is valid if, and only if the unit cell found is PRIMITIVE otherwise it is necessary to convert the unit cell into primitive to calculate the parameters. All the data is refined and converted to CIF file for further data analysis.
From cell refinement general data about the complex is obtained as given below:

Table 5.1

General data of Cu(1)thiourea

Parameter	Description	Parameter	Description
A	13.1305 A°	α	90 °
B	11.2192 A°	β	110.50 °
C	9.7833A°	γ	90°
Cell volume	1349.91 A^3	Crystal system	Monoclinic P

It is not possible to elucidate the structure on the basis of this information as there are few compounds available on the basis of powder diffraction method in data base. Then there is a possibility from the data in table 5.1 to compare with crystal data to identify the possibility of a complex. Cell volume is the only parameter which is

used to do this job. If this cell volume is compared with those on the data base, there are certain compounds whose cell volume is either the same with this value or mutiple. Some examples from the database are given in the table 5.2.

Table 5.2.

Comparison of compound from database on the basis of cell volume

Identifier	Authors	Cell Volume	Formula	Literature reference
SEFJOD	T.S. Lobana, Rekha, R.j. Butcher, A. Castineiras, E. Bermejo, P.V. Bharatam	1344.85	$C_{52}H_{48}C_{12}Cu_2N_6P_2S_2,2(C_2H_3N)$	Inorg. Chem.:45,1535,**(2006)**
WUDFUX	G.A. Bowmaker, N. Chaichit, J.V. Hanna, C. Pakawatchai, B.W. Skelton, A.H. White	2764.93	$C_{52}H_{48}C_{12}Cu_2N_8S_4,2(C_2H_3N)$	Dalton Trans.:8308, **(2009)**
ABALUL01	M. Wriedt, I. Jess, C. Nather	2966.31	$C_{20}H_{20}C_{16}Cu_6N_4S_4$	Private communication, **(2007)**
PAPBIR	Y. Jeannin, F. Secheresse, S. Bernes, F. Robert	2797.3	$3(C_{12}H_{28}N+),C_{15}Cu_4S_4W_3-$	Inorg. Chem.:45,1535,**(2006)**
RAVHOM	Z.A. Saveleva, S.A. Popov, L.A. Glinskaya, R.F. Klevtsova, E.G. Boguslavsky, A.V. Tkachev, S.V. Larionov	1400.19	$C_{20}H_{30}C_{12}Cu_2N_6O_4S_2$	Zh. Strukt. Khim. (Russ.), J. struct. Chem.:46,124,**(2005)**

It can be concluded that the compound belongs to the same category of the compounds in which copper appears as Cu (I). However this research is limited up to this step.

5.6 Summary

The complex was synthesised under mild conditions and at very low concentrations. A white powder is yielded as a result of the reaction between cuprous chloride and thiourea in equal mole ratio (1:1) in methanol. This powder is analysed by powder diffractometer to identify the compound as discussed above. Unfortunately we are limited to this level. Further work is required for this compound. By changing the condition of the solvent, change in molar ratio can provide better result and helpful to identify the compound. It is also possible by dissolving the powder of Cu-thiourea in different solvents can provide the crystals of the compound of different morphology which can be analysed by single crystal X-ray diffraction.

Chapter 6

6.1. Conclusion

6.2. Future Work

6.3. Limitations

6.4. Appendices

6.5. References

6.6. Bibliography for General Reading

6.7. Bibliography for Software

Conclusion

The current research work extends our knowledge of the complex chemistry of coinage metals with substituted thioureas. The structural diversity of such complexes was initially revealed by crystallographic methods and these are the techniques that have been used in this study. Powder XRD has been used in the initial search for novel complexes and this has been followed up by single crystal method to elucidate the full crystal structures.

It is concluded that the synthesis under mild conditions and at low concentration affects the formation of the products. These conditions affect the bonding between the compound and their structural formation.

The use of low molar concentration for reaction of copper(I)chloride with 3-methylbenzothiazole-2-thione in 2:1 molar ratio (M:L) in methanol has yielded a dimer but already synthesis of polymer was isolated only by the change in condition[22]. There is no reaction available between Ag-mbtt under the above conditions. Only mbtt solution is used over Ag solution to study the rearrangement of mbtt under normal condition. In spite of these there is a formation of polymer where silver acts as a bridge in the polymer. Similarly the effect of bi-pyridole on Cu-thiourea has been examined where copper only forms copper sulphate and nitrogen in the ring is replaced by sulphur.

Finally, the variable bonding behaviour between coinage metal and substituted thiourea and the nature of thio-ligand were studied as well as their structural aspects.

The results of the present work propose that the intermolecular interactions like hydrogen-bonding or Pi-Pi stacking interactions in the metal(I)- complexes influence not only the structure of the complexes but also their composition.

Future Work

My current work consists of X-ray diffraction techniques. It contains both single-crystal x-ray diffraction and x-ray powder diffraction. I have discussed some of my newly prepared structures based on these techniques. I left the remaining compounds for future work.

In future I plan to start my work again from this step by changing the conditions and concentrations at a very low level. I would like to change the ligand and metals to view the effect of the coordination between the two.

I will complete the characterization of the compounds prepared on the basis of x-ray diffraction techniques. After this I intend to publish as many of these structures as possible.

Limitations

All of the complexes synthesised were utilized in the crystallographic analysis. Work regarding making more stable complexes is required before their true efficiency can be elucidated. Further work might focus on the synthesis and crystallographic study of complexes with higher molecular weight.

One area that could be applied to the furthering of such X-ray diffraction systems might be to take a combinatorial approach. This has been used, with great effectiveness, in analytical research for many years. With regards furthering the work initiated in this project, a library of structurally related, but subtly different compounds could be established. With the advent of the very fast single crystal structure determination (ca. 20 hours to obtain a basic structure) the department now possesses, the time involved in creating structural libraries are now so low that they are not prohibitive. Such a library would be of great help to study the interactions of different compounds with each other and with new complexes, hence creating lots of new opportunities.

Another area that has relevance to furthering this work is the recent strides made the availability of low cost, powerful computing, CAD, computer aided design, is used extensively throughout the analytical world for rapid development of target system. The results of the CAD experiment can then be fed into the combinatorial library of structures, this information then being used to influence the selection of the test compounds.

Appendices

The whole dissertation is electronically composed using MS office on a standard format.

The general diagrams are made on CHEMDRAW. These figures are then refined and cut and pasted by using snipping tool.

The crystallographic data tables of all complexes 1-4 are generated by using publCIF software. These data tables are refined and pasted in the proper places by using snipping tools.

Structures of the complexes 1-3 are refined by using MERCURY/ORTEP software.

All relative graphs are generated either direct from X-ray powder diffractometer or generated in MERCURY Software for complexes 1-3. These graphs are cut by snipping tools and pasted on the relative places as required.

As such readers wishing to view CIF files for complexes 1-4 are directed to e-mail the author directly using the following address:

amjad.amjad@postgrad.manchester.ac.uk

The author will be happy to supply the enquirer with CIF files in electronic format via an e-mail attachment.

Alternatively, the X-ray department head can be contacted via:

Robin.pritchard@manchester.ac.uk

References

1. P. Aslanidis, S. Divanidis, P.J. Cox, P. Karagiannidis, *Ploy*hedron;* vol. 24, 853-863, **(2005)**.
2. T.S. Lobana, R. Sharma, G. Hundal, R.J. Butcher, *Inor. Chem.*, vol. 45, 9402-9409, **(2006).**
3. T.S. Lobana, R. Sultana, G. Hundal, R.J. Butcher, *Dalton Trans*.; vol. 39, 7870-7872, **(2010).**
4. T.S. Lobana, R. Sultana, G. Hundal, A. Castineiras, *Polyhedron;* vol. 28, 1573-1577. **(2009)**.
5. T.S. Lobana, G. Hundal, *J. Chem. Soc., Dalton Trans.;* 2203, **(2002).**
6. T.S. Lobana, R. Sharma, E. Bermejo, A. Castineiras, *Inor. Chem.;* 42, 7728, **(2003).**
7. A.I. Vogel, *Practical organic chemistry*, P.428; **5th ed.**
8. N.A. Barnes, S.M. Godfrey, R.G. Pritchard, S. Ratcliffe; *Polyhedron;* 29(7), 1822-1832; **(2010).**
9. https://digitalarchive.wm.edu/bitstream/handle/10288/480/Thesis+final.pdf?sequence=1
10. J.S. Lee, R.J. De Angelis, *X-Ray Diffraction Patterns from Binary Nanostructured Materials*, NanostructuredA4ateriaZs, 7, 805-8 12, **(1996).**
11. A.R. West, *Solid State Chemistry and its Applications*, Wiley, NY **(1984).**
12. C.R. Nave. Bragg's Law. *Hyper Physics*, Georgia State University, **(2008).**
13. A.L. Patterson, *Phys. Rev.* 46, 372-376, **(1934).**
14. A.L. Patterson, *Z.* Kristallogr. *Phys. Rev.* 90, 517–542, **(1935).**
15. L.J. Farrugia, J. Appl. Crystallogr. *ORTEP3 for Windows*, 30, 565, **(1997).**
16. SERC@ Carleton College (*http://serc.carleton.edu*)
17. *Organometallic Chemistry*, The Royal Society of Chemistry, Vol. 26, **(1998).**
18. P. Blondeau, A. V. Lee, M, Barboiu, *Inorg. Chem.*, (**2005).**
19. A. Bigotto, B. Pergolese, *Journal of Raman Spectroscopy* Vol. 34, 84–89, **(2003).**
20. L.M. Potikha, A.R. Turelyk, V.A. Kovtunenko, A.V. Turov, O.V. Shishkin, G.V. Palamarchuk, R.I. Zubatyuk, *Chemistry of Heterocyclic Compounds,* **(2010).**

Bibliography for General Reading

21. M.A.S. Goher, F.A. Mautner, *Polyhedron* 18, 1805, **(1999).**
22. W. Clegg, *Crystal Structure Determination*, Oxford University Press, **(1998).**
23. J.E. Huheey, E.A. Keiter, R.L. Keiter (Eds.), *Inorganic Chem.: Principles of Structure and Reactivity*, 4th ed., NY, **(1993).**
24. B, Omar, P.D. Boyle, J. Christie, T. Dyer, S.M. Godfrey, I.R. Howson, C. McArthur, R.G. Pritchard, G.R. Williams *J. Chem. Soc., Dalton Trans.*,3106-3112 **(2000).**
25. S. Ahmad, A. Hussein, A. Isab, P. Herman, Perzanowski, *Transition Metal Chemistry*, 27, 782-785, **(2002).**
26. F.A. Cotton, G.Willkinson, Adv. *Inorganic Chemistry;* Willey & Sons (**1988).**
27. C. Hammond, *The Basics of Crystallography and diffraction*, 2nd Ed., Oxford University Press. **(2001).**
28. G. Brauer, *Handbook of Preparative Chemistry*, 2nd ed., vol. 2, Academic Press, New York, **(1965).**
29. G. Svehla, *Vogel's Qualitative Inorganic Analysis*, 6th ed., **(1979).**
30. R. West, *Solid State Chemistry and its Applications*, Wiley, New York (**1984).**
31. Lectures and class notes by *Dr. Robin Pritchard* (**2010-2011**) unpublished work.
32. A. Castineiras, T.S. Lobana, Rimple, P. Turner, *Inorganic Chem.*, 42 (**2003).**
33. J. Zhang, R.G. Xiong, J.L. Zuo, X.Z. You, *Chem. Commun*. 1495, **(2000).**
34. A. Fortin, M. Drouin, P.D. Harvey, *Inorganic Chem.*, 39, 2758, **(2000).**
35. G.E. Macial, J. J. Ackerman, P. M. Henrichs, *J. Am. Chem. Soc*., **(1977).**
36. J.M. Chow, K.A. Poschmann, N.S. Persky, N.N. Lacuesta, S.L. Stoll, S.G. Bott, S. Obrey, *Inorganic Chem.*, 40, 29, **(2001).**
37. O.R. Evans, W.B. Lin, *Acc. Chem. Res*. 35,511, **(2002).**
38. T.S. Lobana, R. Sharma, G. Hundal, R.J. Butcher, *Inorganic Chem.:* 45 (**2006).**
39. T.S. Lobana, R. Sharma, R. Sharma, S. Mehra, A. Castineiras, P. Turner, *Inorganic Chem.*, 44,1914, **(2005).**
40. M.G. Rossmann, E. Arnold. Intern. *Tables for Crystallography*, Vol. B, 235-263, **(2006).**

Bibliography for Software

41. A. L. Spek, PLATON, *Acta Crystallogr*., Sect A, 46, C34, **(1990)**.
42. A.L. Spek, PLATON, *A Multipurpose Crystallographic* Tool, Utrecht University, Utrecht, The Netherlands, **(1998).**
43. Bruker, APEX2 Software, *Bruker AXS Inc*. V2.0-1, Wisconsin, USA, **(2005).**
44. F.H. Allen, O. Kennard and R. Taylor, *CAMBRIDGE DATA BASE, Acc. Chem. Res.* 16, 146-153, **(1983).**
45. G.M. Sheldrick, *Acta Crystallogr*., Sect. A 64, 112, **(2008).**
46. G.M. Sheldrick, SADABS. Program for Empirical Absorption Correction of Area Detector Data, University of Goettingen, Germany, **(1997).**
47. G.M. Sheldrick, SHELXS97, *Acta Cryst* A, A64, 112-122, **(2008).**
48. I. J. Bruno, J. C. Cole, P. R. Edgington, M. K. Kessler, C. F. Macrae, P. McCabe, J. Pearson and R. Taylor, MERCURY, *Acta Crystallogr*., B58, **(2002).**
49. L.J. Farrugia, WINGX, *J. Appl. Cryst*., 32, 837-838, **(1999).**
50. S. R. Hall, F. H. Allen and I. D. Brown, CIF FORMAT, *Acta Crystallogr*., Sect A, 47, 655-685, **(1991).**
51. S.P. Westrip, publCIF: **(2008).**

+